



TALLINN UNIVERSITY OF TECHNOLOGY  
SCHOOL OF ENGINEERING

---

Department of Materials and Environmental Technology

## Fibrous Silicon Nitride Network of Multi-Axis Architecture

Mitmesuunalise Arhitektuuriga Fiibriline Silikoon Nitriidi Võrgustik

MASTER THESIS

Student	Le Liu
Student code	156319 KAYM
Supervisor	Prof. Irina Hussainova
Co-supervisor	Dr. Marina Aghayan

Tallinn, 2017

## AUTHOR'S DECLARATION

Hereby I declare, that I have written this thesis independently.  
No academic degree has been applied for based on this material.  
All works, major viewpoints and data of the other authors used in this thesis have been referenced.

“.....” ..... 201.....

Author: .....  
/signature /

Thesis is in accordance with terms and requirements

“.....” ..... 201....

Supervisor: .....  
/signature/

Accepted for defence

“.....” .....201... .

Chairman of theses defence commission: .....  
/name and signature/



TALLINNA TEHNIKAÜLIKOOL  
INSENERITEADUSKOND

---

Materjali ja keskkonnatehnoloogia instituut

## Mitmesuunalise Arhitektuuriga Fiibriline Silikoon Nitriidi Võrgustik

Fibrous Silicon Nitride Network of Multi-Axis Architecture

MAGISTRITÖÖ

Üliõpilane: Le Liu

Üliõpilaskood: 156319KAYM

Juhendaja: Prof. Irina Hussainova

Kaasjuhendaja: Dr. Marina Aghayan

Tallinn, 2017.a.

## AUTORIDEKLARATSIOON

Olen koostanud lõputöö iseseisvalt.

Lõputöö alusel ei ole varem kutse- või teaduskraadi või inseneridiplomit taotletud. Kõik töö koostamisel kasutatud teiste autorite tööd, olulised seisukohad, kirjandusallikatest ja mujalt pärinevad andmed on viidatud.

“.....” ..... 201.....

Autor: .....  
/ allkiri /

Töö vastab bakalaureusetöö/magistritööle esitatud nõuetele

“.....” ..... 201.....

Juhendaja: .....  
/ allkiri /

Kaitsmisele lubatud

“.....” .....201... .

Kaitsmiskomisjoni esimees .....  
/ nimi ja allkiri /

# TABLE OF CONTENTS

1. INTRODUCTION.....	8
2. REVIEW OF LITERATURE.....	9
2.1 The structure of Si <sub>3</sub> N <sub>4</sub> .....	9
2.2 The applications of Si <sub>3</sub> N <sub>4</sub> .....	10
2.2.1 Si <sub>3</sub> N <sub>4</sub> bulks.....	10
2.2.2 Si <sub>3</sub> N <sub>4</sub> fibers .....	11
2.3 Fabrication of Si <sub>3</sub> N <sub>4</sub> .....	11
2.3.1 Synthesis of Si <sub>3</sub> N <sub>4</sub> powders .....	11
2.3.2 Synthesis of Si <sub>3</sub> N <sub>4</sub> fibers.....	12
2.3.3 Production of Si <sub>3</sub> N <sub>4</sub> bulks.....	16
2.4 Introduction to Selective Laser Sintering .....	16
2.4.1 Overview of additive manufacturing .....	16
2.4.2 Overview of selective laser sintering .....	17
2.5 Objectives of the study .....	18
3. EXPERIMENTAL .....	19
3.1 Preparation of Si <sub>3</sub> N <sub>4</sub> network .....	19
3.1.1 Catalyst preparation.....	19
3.1.2 Fabrication of fibrous Si <sub>3</sub> N <sub>4</sub> networks by die pressing and direct nitridation .....	20
3.1.3 Fabrication of fibrous Si <sub>3</sub> N <sub>4</sub> networks by SLS and direct nitridation.....	21
3.2 Characterization.....	23
4. RESULTS AND DISCUSSION .....	25
4.1 The effect of catalyst .....	25
4.1.1 The effect of catalyst on direct nitridation process.....	25
4.1.2 Influence of the nitridation atmosphere.....	31
4.2 Fibrous silicon nitride network with complex geometry.....	33
4.2.1. Selective laser sintering of silicon.....	33
4.2.2 Nitridation of shaped silicon samples.....	35
4.3 Mechanical properties and thermal stability of fibrous Si <sub>3</sub> N <sub>4</sub> network .....	37
4.3.1 Mechanical properties of Si <sub>3</sub> N <sub>4</sub> network .....	37
4.3.2 Thermal stability of Si <sub>3</sub> N <sub>4</sub> network.....	38
4.4 Si <sub>3</sub> N <sub>4</sub> fiber.....	38
4.4.1 Morphology of Si <sub>3</sub> N <sub>4</sub> fiber .....	38
4.4.2 Composition of Si <sub>3</sub> N <sub>4</sub> fiber.....	40

4.4.3 Thermal stability of Si <sub>3</sub> N <sub>4</sub> fiber .....	40
CONCLUSIONS .....	42
RÉSUMÉ.....	43
RESÛMEE .....	44
REFERENCE .....	45
ACKNOWLEDGEMENTS .....	50

## **List of Abbreviations and symbols**

1D – One dimensional

DSC – Diffraction scanning calorimetry

MNF – Mullite nanofibers

ONH – Oxygen/Nitrogen/Hydrogen analyzer

SEM – Scanning electron microscope

SLM – Selective Laser Melting

SLS – Selective Laser Sintering

STA – Simultaneous thermal analysis

TG – Thermogravimetry

vol.% – Volume percentage

wt.% – Weight percentage

XRD – X-ray diffraction

# 1. INTRODUCTION

As a key industry material, silicon nitride ( $\text{Si}_3\text{N}_4$ ) was discovered in 1857 and became commercialized since 1950's [1].  $\text{Si}_3\text{N}_4$  based materials are widely used in a variety of areas such as in heat exchanger bearings, chemical reaction vessels, high-temperature components, automotive parts, and in aerospace fields [2-4]. This broad interest towards silicon nitride arises from a favorable combination of its outstanding properties such as great hardness, wear resistance, chemical stability, low density, and high mechanical strength, etc. [5].  $\text{Si}_3\text{N}_4$  can withstand very harsh environments where metals and polymers fail [2].

While in recent years fibrous  $\text{Si}_3\text{N}_4$  with high porosity also draw people's attention [6], as the nest-like structure of network possess combination of advantages, including low density, high thermal shock resistance, high mechanical strength, and possible electrical conductivity. In the past 10 years, porous  $\text{Si}_3\text{N}_4$  gained new wave of attention as bio-structural material due to its excellent biocompatible, bioactive properties [4]. As a relatively new biomaterial, silicon nitride has been currently used as arthrodesis device material [6] and spinal implant material [7]. In 2011, the first silicon nitride femoral heads were implanted [8].

However, manufacturing of silicon nitride components with net-shape is difficult because of strong covalent Si-N bonds hindering mass transport through grain-boundary, and, therefore, arises many economical, ecological and engineering problems. Usually, die pressing is the easiest way of producing simple shape components; slip casting and injection molding are favored to produce complex structured ceramic components. These techniques require admixtures, binders, which should be burnout carefully taking hours, even days [5]. These time-consuming manufacturing processes may terminate the application of this materials, since smart, rapid technologies, such as additive manufacturing(AM), have being developed.

Nowadays, additive manufacturing gives new opportunities to produce complicated shaped materials. Selective Laser Sintering (SLS) is one of the most commercialized additive manufacturing method [9]. It allows for the direct manufacturing of complex end-use parts and facilitates tooling for conventional manufacturing technologies, reducing costs and lead times [9]. Whereas, till now there is limited successful attempt to produce near-net-shape  $\text{Si}_3\text{N}_4$  components by SLS.

In this work, it is proposed to prepare  $\text{Si}_3\text{N}_4$  by two steps: (i) preparation of the green body of silicon with designed geometry, (ii) reactive sintering to form bulk  $\text{Si}_3\text{N}_4$  by direct nitridation.

## 2. REVIEW OF LITERATURE

### 2.1 The structure of Si<sub>3</sub>N<sub>4</sub>

Pure silicon nitride is a white, high-melting-point solid (the main properties are listed in Table 2.1). It has excellent thermal shock resistance and high-temperature strength due to its unique structures.

Table 2.1 Silicon nitride properties [10]

Silicon nitride properties	Value
Chemical formula	Si <sub>3</sub> N <sub>4</sub>
Molar mass	140.28 g·mol <sup>-1</sup>
Appearance	Grey, odorless powder
Density	3.2 g/cm <sup>3</sup> , solid
Melting point	1900 °C; (decomposes)
Solubility in water	Insoluble

There are three crystallographic structures of silicon nitride (Si<sub>3</sub>N<sub>4</sub>), designated as  $\alpha$ ,  $\beta$  and  $\gamma$  phases [10]. The  $\alpha$  and  $\beta$  phases are the most common forms of Si<sub>3</sub>N<sub>4</sub>, and can be produced under ordinary pressure condition. The  $\gamma$  phase can only be synthesized under high pressures (17 GPa) and temperatures (2100 K) [11].

The  $\alpha$  and  $\beta$ -Si<sub>3</sub>N<sub>4</sub> have hexagonal structures, which are built up by corner-sharing SiN<sub>4</sub> tetrahedra [12]. They can be regarded as consisting of layers of silicon and nitrogen atoms in the sequence ABAB... or ABCDABCD... in  $\alpha$ -Si<sub>3</sub>N<sub>4</sub> and  $\beta$ -Si<sub>3</sub>N<sub>4</sub>, respectively. ABCDABCD... in  $\alpha$ - Si<sub>3</sub>N<sub>4</sub> and  $\beta$ - Si<sub>3</sub>N<sub>4</sub>, respectively (Fig. 2.1 a and b). The AB layer is the same in the  $\alpha$  and  $\beta$  phases, and the CD layer in the  $\alpha$  phase is related to AB by a c-glide plane. The SiN<sub>4</sub> tetrahedra in  $\beta$ - Si<sub>3</sub>N<sub>4</sub> are interconnected that tunnels are formed, running parallel with the c axis of the unit cell.

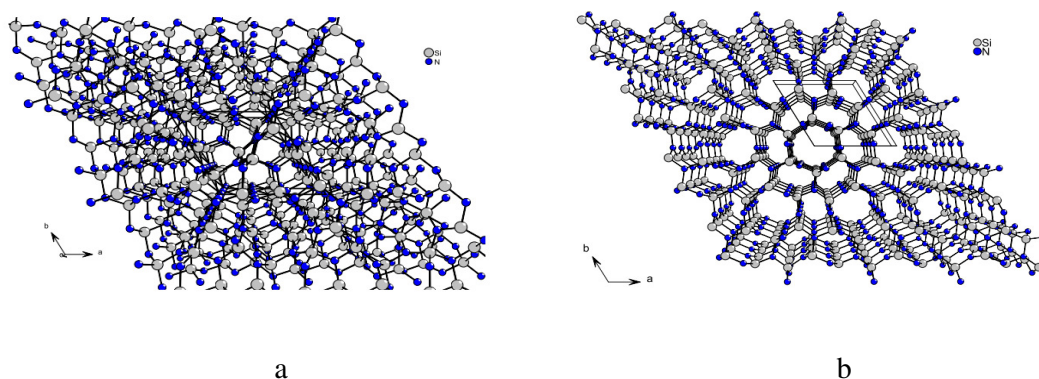


Figure 2.1 Crystal structure stacking model of a)  $\alpha$ - Si<sub>3</sub>N<sub>4</sub>, b)  $\beta$ - Si<sub>3</sub>N<sub>4</sub> [13]

This rigid structure and strong covalent bonds are the cause of the extraordinary hardness, durability, and mechanical strength of this material [5].

## 2.2 The applications of $\text{Si}_3\text{N}_4$

### 2.2.1 $\text{Si}_3\text{N}_4$ bulks

Discovered in 1857, the  $\text{Si}_3\text{N}_4$  remained merely a chemical curiosity for decades before usage in commercial applications [14]. Since 1953, the research aimed at high-temperature parts of gas turbines has resulted in the development of a reaction-bonded silicon nitride and a hot-pressed silicon nitride [14]. Then gradually it was in commercial production for thermocouple tubes, rocket nozzles and crucibles for melting metals.

Since 1990, the cost has been reduced substantially as production volume has increased [15]. The wear resistance, low friction, high stiffness, and low density of  $\text{Si}_3\text{N}_4$  has led to the development, in the sintered form of high-temperature unlubricated roller and ball bearings. Low friction and rolling contact fatigue rate gives  $\text{Si}_3\text{N}_4$  bearings longer life than conventional higher-density steel and hard-metal bearings. Applications also include the bearings in oil drills, vacuum pumps, and unlubricated dental drills [15].



Figure 2.2  $\text{Si}_3\text{N}_4$  components (a) used in automobile industry [16]; (b) bioscaffolds [8].

The largest market for  $\text{Si}_3\text{N}_4$  components is in (diesel and spark-ignited) engines in automobile industry (Fig. 2.2(a)) [10]. Most of these components are manufactured in the United States and Japan, although considerable development work also has been conducted in Germany and other European Union countries [10].

Recently, silicon nitride is used as an orthopaedic biomaterial, to promote bone fusion in spinal surgery and to develop bearings that can improve the longevity of prosthetic hip and knee joint [17]. Cervical spacers and spinal fusion devices made of silicon nitride composites are presently in use (Fig. 2.2(b)), with successful clinical trials [17].

## 2.2.2 Si<sub>3</sub>N<sub>4</sub> fibers

One dimensional ceramics show unusual mechanical strength. Therefore, the use of ceramic whiskers, fibers are desirable reinforcing agent for development of high performance composite materials [18]. For example, SiC and Al<sub>2</sub>O<sub>3</sub> whiskers were widely studied because of high specific strength, specific stiffness, relatively low specific weight, high corrosion and erosion resistance [19,20].

However, Si<sub>3</sub>N<sub>4</sub> fibers are not widely used although they exhibit outstanding properties such as tensile strength (30-50 GPa) [21], good electrical insulating properties at elevated temperatures and low dielectric constant [22]. It is because there are still problems in producing pure and uniform whiskers/fibers on a large scale in an economical way, moreover to incorporate them into matrix [18]. The development of economic production of fiber-reinforced composites may open new application.

Furthermore, potential hazard arising from asbestos fibers is one more challenge that repels the usage of ceramics fibers. Thus, the health precautions should be taken into account while suggesting a complex processing: from synthesis to application [19].

## 2.3 Fabrication of Si<sub>3</sub>N<sub>4</sub>

### 2.3.1 Synthesis of Si<sub>3</sub>N<sub>4</sub> powders

There are three main methods and several unpopular methods used for the production of Si<sub>3</sub>N<sub>4</sub> powders:

#### 1) Carbothermal reduction method

The carbothermal reduction of SiO<sub>2</sub> powder under nitrogen (that is, by heating silica, carbon in nitrogen at 1250–1300 °C) was the earliest used method for Si<sub>3</sub>N<sub>4</sub> production [23].



This method is now considered as the most-cost-effective industrial route for the production of high-purity  $\alpha$ -Si<sub>3</sub>N<sub>4</sub> powder.

#### 2) Direct nitridation method

The Si<sub>3</sub>N<sub>4</sub> powders can be prepared by heating powdered silicon between 1300 °C and 1400 °C in an atmosphere of nitrogen [24]:



During the reaction, the silicon sample weight increases progressively due to the chemical combination of silicon and nitrogen. Without a catalyst, the reaction is complete after several hours (~7), when no further weight increase due to nitrogen absorption is detected [24]. Some

metal, such as Ni, Co, Cu, Ca, Fe, Y, Cr, W, Ag and Al had been used as catalyst on direct nitridation of silicon [25-28].

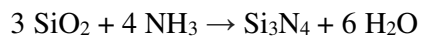
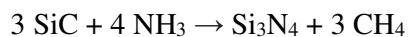
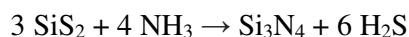
### 3) Silicon amide method

The development of the long-known but little-used silicon amide route relied on the increased availability of low-cost silicon tetrachloride (SiCl<sub>4</sub>). Silicon diimide (Si(NH)<sub>2</sub>) decomposition gives initially amorphous Si<sub>3</sub>N<sub>4</sub>, which is converted to the α-Si<sub>3</sub>N<sub>4</sub> form by heating under nitrogen at 1400°C–1500°C [5].



### 4) Other methods

Several other reactions of producing silicon nitride [5] have not gained importance for technological or economic reasons, such as too expensive, too slow reaction kinetics, or the development of undesirable particle morphologies.



## 2.3.2 Synthesis of Si<sub>3</sub>N<sub>4</sub> fibers

In recent years, Si<sub>3</sub>N<sub>4</sub> fibers were synthesized by employing different routes (Table 2.2). Although different approach in detail, most of them based on the similar process. For example, they need silicon or silicon contained materials as precursor, metal or metal oxide as catalyst, reacted with N<sub>2</sub> or NH<sub>3</sub> at high temperature (1000°C-1450°C). The growth processes of the fibers with and without particles (caps or droplets) at their tips were explained by vapor–liquid–solid (VLS) and vapor–vapor–solid (VVS) mechanisms respectively.

Table 2.2 Synthesis methods of silicon nitride fibers

No.	Authors	Raw material	Synthesis method	Gas	Temperature	Fiber Diameter	Potential application
1	Seiji Kamimura et al. [29].	Polycarbosilane (PCS) fiber	1.Irradiation with electron beams (EB). 2.The cured PCS fiber was heated up to 1000°C in NH <sub>3</sub> gas atmosphere. 3.heat treatment in nitrogen gas	NH <sub>3</sub> N <sub>2</sub>	500-1000°C (the reaction starts at around 500°C and terminates at about 700°C.)	14-15 μm	high-temperature electric wire insulator
2	Xin Xu et al. [30].	A mixture of silica gel and Si (molar ratio of 1:1) mixed with Fe powder together	1400°C in a vertical induction furnace, nanowires were collected on a graphite susceptor cover	N <sub>2</sub> /NH <sub>3</sub> gas flow 5:1	1400°C	100-200 nm	miniature electronic and photonic devices, solar cell and photoelectrical diode
3	Zhihao Wang et al. [31].	silicon powder (200 mesh, 99.9%), 8% lanthanum (99.9%)	1350°C for 4 h. N <sub>2</sub> at a flow rate of 50 sccm. Products were obtained in the alumina crucible	N <sub>2</sub>	1350°C	30–40 nm	host material for high temperature and radiation environment with high doping concentration
4	Yingjiu Zhang et al. [32].	Si powders or Si/SiO <sub>2</sub> mixtures (less than 74 μm) with or without metal catalyst	The mixtures were heated at 1200°C for 60 min. layer was found on the surfaces of the mixtures and the Al <sub>2</sub> O <sub>3</sub> boats	N <sub>2</sub> , Ar and NH <sub>3</sub>	1200°C	10–70nm and 10–300 nm, respectively	high strength, light weight, good resistance to thermal shock and oxidation.
5	Mashkoor AHMAD et al. [33].	1.Si substrates, Ga and Ga <sub>2</sub> O <sub>3</sub> (4:1) 2. Si substrates, Fe rod.	two alumina boats placed inside a quartz tube, Si substrates was put in the top of alumina crucible	NH <sub>3</sub>	1050°C	30–100 nm	optoelectronic nanodevices
6	Karine Saulig-Wenger et al. [34].	silicon powder (99.999%) and a piece of graphite	placed in the alumina tube of a horizontal tubular furnace, held for 1 h	N <sub>2</sub>	1300°C	10 to -300 nm	nanoelectronics

No.	Authors	Raw material	Synthesis method	Gas	Temperature	Fiber Diameter	Potential application
7	Feng Liang et al. [35].	1.25-5 wt% Cr, Si (99.9% pure, $\leq 44 \mu\text{m}$ )	1. 30 min in a ball mill 2. 1200–1350 °C for 3 h in flowing N <sub>2</sub>	N <sub>2</sub>	1350 °C	50–200 nm, 50 $\mu\text{m}$ in length	excellent thermal shock resistance, mechanical properties and chemical stability
8	Xiaoguang Zhang et al. [36].	Si, SiO <sub>2</sub> , PEG with an average molecular weight of 4000	ultrasonic cell disruptor, After Si <sub>3</sub> N <sub>4</sub> nanowires were well dispersed in absolute ethanol, PEG was added into the beaker, dried in a drying oven at 60°C for 30 min	N <sub>2</sub>	1450 °C	400 nm	PCMs (phase-change materials) have been widely utilized in air-conditioning systems, portable electronics, building energy conservation, temperature-controlled green houses and solar heating systems, as well as can be integrated into hybrid vehicles
9	Feng Wang et al. [37].	Phenolic resin, tetraethoxysilane, ferric nitrate, ethanol, oxalic acid	carbonaceous silica (C-Si) sol was heated in 1100–1300°C, 1–30 h	N <sub>2</sub>	1100–1300 °C	Nano level	reinforcements in ceramic-matrix composites
10	Ji-Xuan Liu et al. [38].	Si (20 $\mu\text{m}$ ), h-BN (1 $\mu\text{m}$ ), organic additives	ball mixed, graphite resistance furnace	N <sub>2</sub>	1450°C	60–300 nm	radomes and antenna windows
11	Gong-Yi Li et al. [39].	SiO <sub>2</sub> powders and short carbon fibers	Heating Csf/SiO <sub>2</sub> composites at 1430°C for 2 h in a flowing	N <sub>2</sub>	1430°C	70–300 nm, length is up to 1–2 mm	wide band semiconductor at both ambient and elevated temperatures
12	Mashkooor Ahmad et al. [40].	Si with Ni coated as catalyst, Ga	Ga as source material was placed in the central region of the quartz tube furnace. Si substrate was loaded on the top of the alumina boat. kept for 3 h under a constant flow.	ammonia	900–1200 °C	30–100 nm	the integration of future novel nanodevices and nanocomposites

No.	Authors	Raw material	Synthesis method	Gas	Temperature	Fiber Diameter	Potential application
13	Haitao Liu et al. [41].	n-type Si (100) wafer, nickel nitrate	Si (100) wafer with its Ni(NO <sub>3</sub> ) <sub>2</sub> catalyst was separated with another Si source (metallic silicon powder).	without	1150 °C	80 to 150 nm	optoelectronics
14	Qiushi Wang et al. [42].	Si (mean size: 200 mesh), SiO <sub>2</sub> , graphite powders	improved DC arc discharge plasma setup, 100 A, 20V, 6 h.	N <sub>2</sub>		50–200 nm	blue light-emitting devices
15	Juntong Huang et al. [43].	Si and Co	direct nitridation of silicon	N <sub>2</sub>	1300 to 1350 °C	80–120 nm	fracture toughness increases
16	Yajie Xu et al. [44].	amorphous porous silica and activated carbon	carbothermal reduction and nitridation route	NH <sub>3</sub>	1350 °C	600-1200 nm	light and electron emission devices
17	Arik, H., S. Saritas, and M. Gündüz. [45].	sepiolite	carbothermal reduction and nitridation	N <sub>2</sub>	1200 to 1450 °C	0.5–3 μm	high temperature engineering applications

### **2.3.3 Production of Si<sub>3</sub>N<sub>4</sub> bulks**

Pure silicon nitride is difficult to produce no matter as dense or porous type. This covalently bonded material does not readily sinter and cannot be heated over 1850°C which result in dissociation of it to silicon and nitrogen [46].

Dense silicon nitride is normally made using methods that give bonding through indirect methods, such as sintering additives to aid densification. Traditionally, the main approaches to the preparation of dense Si<sub>3</sub>N<sub>4</sub> ceramics is Hot Isostatic Pressing (HIP) or Hot Pressing (HP), which uses Si<sub>3</sub>N<sub>4</sub> powders mixed with a small amount of Al<sub>2</sub>O<sub>3</sub> and Y<sub>2</sub>O<sub>3</sub> as sintering additives [47]. The HIP and HP process subjects a component to both elevated temperature and pressure. HIP can be used to reduce the porosity and increase the density of many Si<sub>3</sub>N<sub>4</sub> based composites. The HP process is similar to HIP, just the pressure is applied from two punches rather than from isostatic gas. To produce dense silicon nitride in quick process, another alternative is Field Assisted Sintering Technique (FAST)/Spark Plasma Sintering (SPS) method [13].

There were also many methods to produce porous silicon nitride materials. Jian-Feng Yang et al. [48] fabricated silicon nitride ceramics of various porosities using a Yb<sub>2</sub>O<sub>3</sub> sintering additive by liquid-phase sintering technique between 1600 and 1850 °C. Zhaoyun Xu et al. [49] synthesized porous silicon nitride ceramics by sintering mixtures containing fibrous and equiaxed a-Si<sub>3</sub>N<sub>4</sub> powder with a various content ratios. Takayuki Fukasawa et al. [50] developed a freeze-drying process to produce porous silicon nitride with macroscopically aligned channels. Firstly, freezing a water-based slurry, then drying the ice, further sintering at around 1800 °C.

## **2.4 Introduction to Selective Laser Sintering**

### **2.4.1 Overview of additive manufacturing**

According to the American Society for Testing and Materials (ASTM), “additive manufacturing” is the “process of joining materials to make objects from 3D model data, usually layer upon layer” [51]. The AM market can be applied in various industries such as motor vehicles, consumer products, business machines, medical, academic, aerospace, government/military, and others (architecture, paleontology, and forensic pathology) [52-54]. Additive manufacturing has a great potential to revolutionize the global parts manufacturing and logistics landscape. It has been recognized as a blasting technology to manufacture

customize designed both geometrically and functionally complex structures (and semifinished parts), moreover it provides unusual regulation of the shape and internal structure of fabricated objects.

AM technology has been used mostly for manufacturing polymeric or metallic materials. In the direct 3D printing methods of ceramics, the high heating and cooling rates cause the brittleness and poor fracture toughness of obtained shapes [55]. And although AM is not in competition with traditional manufacturing methods of ceramics, it steps up new approaches of research and applications.

### 2.4.2 Overview of selective laser sintering

Selective laser sintering is an AM technique that uses a laser as the power source to sinter powdered material [55]. Selective laser sintering is similar to Selective Laser Melting (SLM), the two are instantiations of the same concept but differ in technical details. In SLS, the material is sintered rather than fully melted [56]. The process of SLS/SLM is also known as Laser Beam Melting (LBM) [57], Direct Metal Laser Sintering (DMLS) [58] or Laser Casting [59]. Despite diverse naming, they basically share the same approach [60]: The starting point is a 3D Computer-Aided Design (CAD) model that is created on a computer. The model is virtually sliced into thin layers with a typical layer thickness of  $20\ \mu\text{m} - 1\ \text{mm}$ . Once the powder layer is distributed, a 2D slice is fully melted using a laser beam applied to the powder bed. The melting process is repeated slice by slice, layer by layer, until the last layer is melted and the parts are complete. Then it is removed from the powder bed and post processed according to requirements.

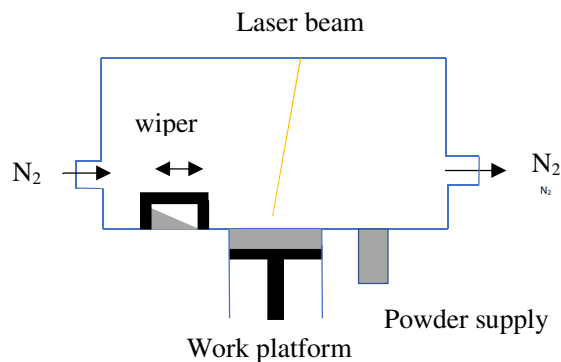


Figure 2.3 Diagram of SLS components

SLS/SLM (Fig. 2.3) is featured by an automatic process used to create both geometrically and functionally complex intricate geometries, end-use parts with good dimensional tolerance [62]. The working process of SLS or SLM process is the following: powder material is applied in thin layers and melted (or sintered) at the predetermined areas using thermal energy supplied through a powerful laser beam. Following the sintering of all selected locations of the target layer, the work platform is lowered, as a result new powder layer can be supplied repeatedly by the wiper, until the complete shape formation of the samples. The experiments can be carried out in nitrogen or argon environment.

## **2.5 Objectives of the study**

This research is motivated by the fact that although silicon nitride was widely used in current industry, it is still difficult to form fibrous silicon nitride network with complex shape. The main objectives of this work are:

- 1) To produce fibrous network of silicon nitride with controlled shape
  - a. To produce the silicon shape by die pressing.
  - b. To optimize the parameters of producing silicon shape by SLS.
  - c. To find effective catalysts for producing fibrous silicon nitride network by direct nitridation method.
- 2) Characterize the as-produced  $\text{Si}_3\text{N}_4$  network
  - a. Morphology by SEM
  - b. Composition by XRD and ONH
  - c. Mechanical properties by compression test
  - d. Thermal stability in air by DSC/TG

### 3. EXPERIMENTAL

#### 3.1 Preparation of Si<sub>3</sub>N<sub>4</sub> network

The network of Si<sub>3</sub>N<sub>4</sub> was produced via direct nitridation of die pressed or SLS-ed Si (particle size <44 μm, purity ≥99%, Whole Win (Beijing) Materials Sci. & Tech. Co., Ltd. China) samples in N<sub>2</sub> (>99.999%) or diluted NH<sub>3</sub> (10 vol. % NH<sub>3</sub> in N<sub>2</sub>) using different catalysts.

##### 3.1.1 Catalyst preparation

Mullite nanofibers (MNF) were used as catalyst support on which MnO, Ce<sub>2</sub>O<sub>3</sub>, Cr<sub>2</sub>O<sub>3</sub>, Co<sub>3</sub>O<sub>4</sub>, NiO and Fe<sub>2</sub>O<sub>3</sub> were deposited by solution combustion method [63]. The raw materials used were list in Table 3.1 along with the description.

Table 3.1 Compound used for preparing catalysts

Compound	Purity	Supplier
Mn(NO <sub>3</sub> ) <sub>2</sub> *4H <sub>2</sub> O	≥98%	Aldrich
Ce(NO <sub>3</sub> ) <sub>3</sub> *6H <sub>2</sub> O	≥98%	Sigma-Aldrich
Cr(NO <sub>3</sub> ) <sub>3</sub> *9H <sub>2</sub> O	≥99%	Honeywell
Co(NO <sub>3</sub> ) <sub>2</sub> *6H <sub>2</sub> O	≥98%	Honeywell
Ni(NO <sub>3</sub> ) <sub>2</sub> *6H <sub>2</sub> O	≥98.5%	Sigma-Aldrich
Fe(NO <sub>3</sub> ) <sub>3</sub> *9H <sub>2</sub> O	≥98%	Sigma-Aldrich
Glycine	≥99%	Sigma

Table 3.2 Composition of reactive solution

Compound	Amount of metal nitrate (g)	Amount of glycine (g)
Mn(NO <sub>3</sub> ) <sub>2</sub> *4H <sub>2</sub> O	2.46	0.82
Ce(NO <sub>3</sub> ) <sub>3</sub> *6H <sub>2</sub> O	8.47	2.44
Cr(NO <sub>3</sub> ) <sub>3</sub> *9H <sub>2</sub> O	7.89	2.47
Co(NO <sub>3</sub> ) <sub>2</sub> *6H <sub>2</sub> O	8.56	2.29
Ni(NO <sub>3</sub> ) <sub>2</sub> *6H <sub>2</sub> O	2.87	0.83
Fe(NO <sub>3</sub> ) <sub>3</sub> *9H <sub>2</sub> O	7.94	2.46

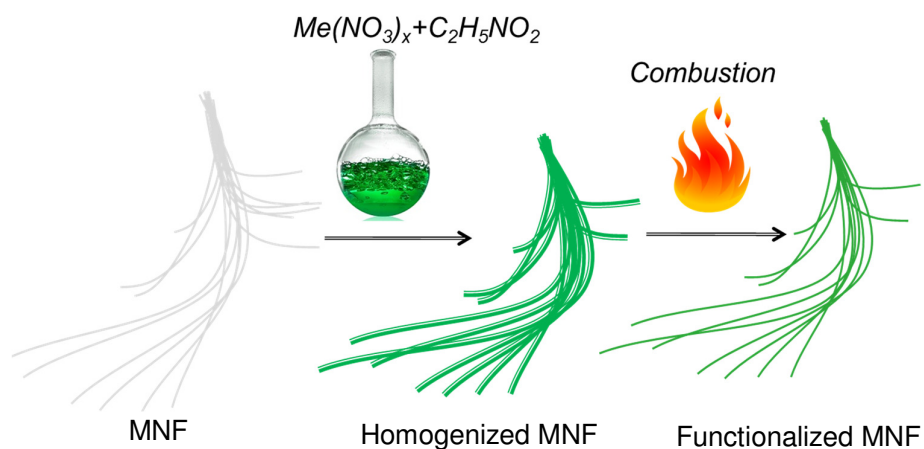


Figure 3.1 Scheme of synthesis of catalysts

Appropriate amount of metal nitrates (Table 3.2) as source of oxidized metal (act as oxidizers) and glycine (as source of energy and reducers) were dissolved in 8 ml of distilled water to prepare reactive solutions (Fig. 3.1). The reactive solutions were soaked by 1g of mesoporous network of MNF, which was aged for 30 minutes to provide homogeneous distribution of the components. Afterwards they were heated at 400°C for 30 minutes in a muffle furnace, where the solution combustion took place. The solution combustion reactions were as follows:



After the solution combustion reactions, metallic oxides distributed on MNF (with 1:1 molar ratio) was obtained. In addition, commercial available nickel nanopowders (particle size <100nm, purity  $\geq 99\%$ , Sigma-Aldrich) were also used as separate catalyst.

### 3.1.2 Fabrication of fibrous $Si_3N_4$ networks by die pressing and direct nitridation

Silicon powder was mixed with 1.5 wt.% of each catalyst and homogenized in ceramic mortar for 5 min. Small amount (with 2:1 weight ratio) of polymer solution ( $\geq 50$  wt. % cycloalkane, LAHUSTI, AS Baltoil, Estonia) was added as binder to make slurry. The slurry was dried in oven at 60 °C for 30 min. Finally, samples with certain shapes (depends on the press mould) for each mixture were made by die pressing (the pressure was about 2 MPa). The entire process was shown in Fig. 3.2.

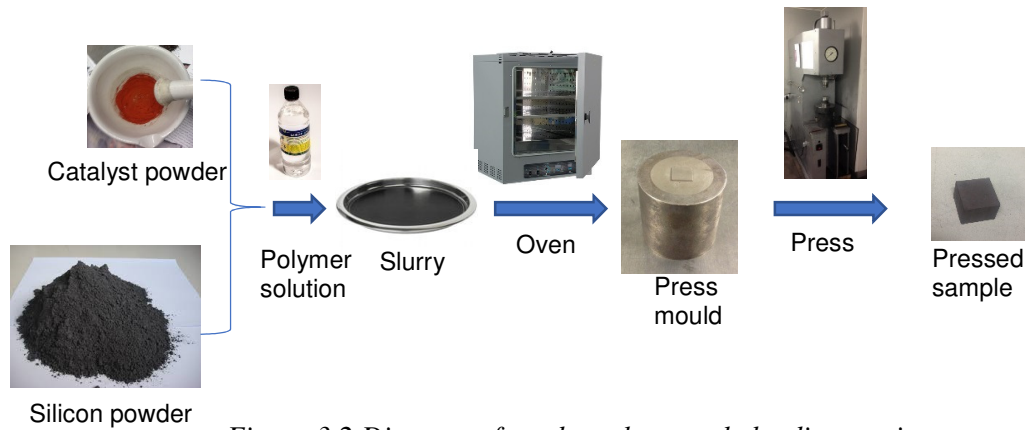


Figure 3.2 Diagram of produce the sample by die pressing

Finally, the samples were heated to 1300 °C at the rate of 10 °C /min under the gas (N<sub>2</sub> or diluted NH<sub>3</sub>) flow of 200 sccm and kept at the temperature for 5 hours. Fig. 3.3 shows the schematic diagram of the experimental apparatus, which mainly consists of a resistance furnace (WEBB, USA), a reaction crucible (diameter 66mm, height 40mm), and a gas supply system.

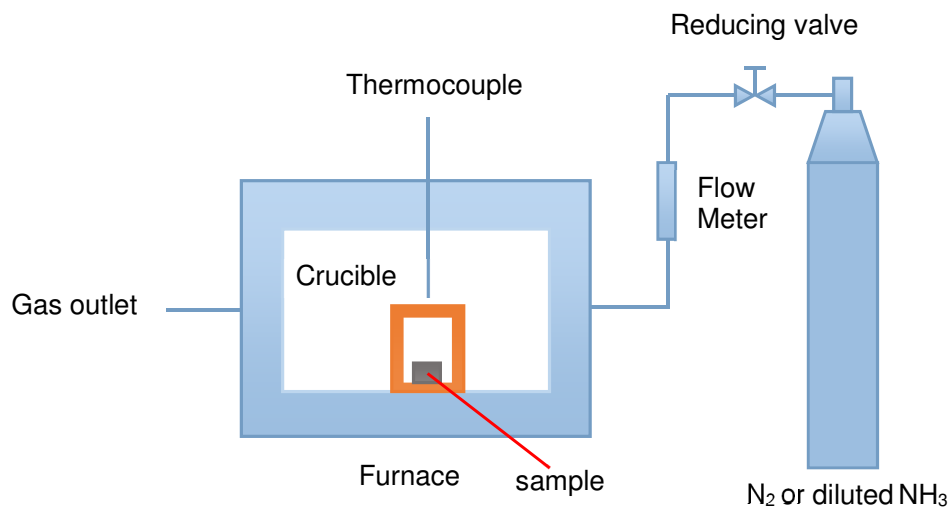
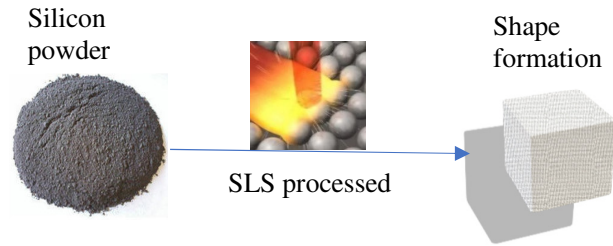


Figure 3.3 Flow diagram of direct nitridation in pressure less furnace

### 3.1.3 Fabrication of fibrous Si<sub>3</sub>N<sub>4</sub> networks by SLS and direct nitridation

The silicon powder (the same as used for die pressing) was chosen as starting material. The silicon powder (with or without catalyst) was 3D printed by SLS/SLM (ReaLizer GmbH, Germany) directly.



*Figure 3.4 Sintering process of silicon powder*

Generally, there are several parameters effecting the sintering process: such as the laser current, point distance and exposure time. Our first task was to find out the parameter with the significant effect on the process. As a result, 18 cubic samples with 5 mm of side length were designed (Fig. 3.4). The exposure time from 125 to 375  $\mu\text{s}$ , point distance from 10 to 30  $\mu\text{m}$ , laser current from 500 to 1100 mA were altered separately to find the best parameter combination on the SLS process (Table 3.3).

*Table 3.3 Samples and reaction parameters*

Sample	Exposure time( $\mu\text{s}$ )	Point distance( $\mu\text{m}$ )	Laser current (mA)
1	125	10	500
2	125	20	500
3	125	30	500
4	250	10	500
5	250	20	500
6	250	30	500
7	375	10	500
8	375	20	500
9	375	30	500
10	125	10	1100
11	125	20	1100
12	125	30	1100
13	250	10	1100
14	250	20	1100
15	250	30	1100
16	375	10	1100
17	375	20	1100
18	375	30	1100

Later, the best catalyst was mixed with the silicon power and 3D printed by SLS with optimized parameters. The obtained samples were finally nitridized in the furnace by the same parameters used in die pressing route.

### 3.2 Characterization

In this study, scanning electron microscopy (SEM) with magnifications up to 10 kX was used for examination of the precursor materials and the final product. Additionally, field emission scanning electron microscopy (FESEM) was used to characterize the microstructure of the fibers, which was before-head coated with gold.

The phase compositions of the powders were analyzed with the help of X-ray diffractometers (XRD). Samples were irradiated with CuK $\alpha$  radiation at 40 kV and 30 mA, in a  $\theta - 2\theta$  scan with a step size of 0.02° and a count time of 0.4 s.

While for precise nitrogen content measurement, the content of nitrogen was analyzed by ONH analyzer. In this analysis, during the heating of the sample in a graphite crucible up to 3000 °C, nitrogen was released in its elemental form. Carbon monoxide was produced by the reaction of carbon in the graphite crucible and oxygen of the sample. The carrier gas (helium) and sample gasses passed through a dust filter before entering a copper oxide catalyst which converts the CO to CO<sub>2</sub>. CO<sub>2</sub> and water were removed chemically and nitrogen concentrations was determined by measuring the thermal conductivity.

For mechanical properties, the compressive strength of fibrous Si<sub>3</sub>N<sub>4</sub> network specimens were measured by Zwick with the speed of 0.127 mm/min (the speed calculated based on ASTM E9/09 [64]). The compressive strength was calculated by the average of seven specimens. While the yield strength was calculated from stress-strain curve.

Furthermore, the thermal stability of the synthesized specimens was analyzed by Diffraction scanning calorimetry/Thermogravimetry (DSC/TG). Simultaneous thermal analysis (STA) of fibrous Si<sub>3</sub>N<sub>4</sub> network and Si<sub>3</sub>N<sub>4</sub> fibers were made in flowing air (20 mL/min) and 10 °C /min heating rate up to 1470°C in open alumina crucibles.

All the characterization methods are listed in Table 3.4.

*Table 3.3 Methods used for characterization of fiber-reinforced Si<sub>3</sub>N<sub>4</sub> and Si<sub>3</sub>N<sub>4</sub> fibers*

Characterization methods	Properties	Apparatus
SEM	Morphology, particle size	Hitachi TM-1000, Japan
FESEM	Fiber diameter	FESEM S-4700, Hitachi, Japan
XRD	Phase composition	Bruker D5005, USA
ONH	Elemental composition	Eltra, Germany

Compression test	Mechanical properties	Laboratory of Mechanical Testing and Metrology, TTU. Zwick, Germany
DSC/TG	Thermal stability	STA 449C Jupiter, Netzsch-Gerätebau GmbH, Germany

## 4. RESULTS AND DISCUSSION

### 4.1 The effect of catalyst

#### 4.1.1 The effect of catalyst on direct nitridation process

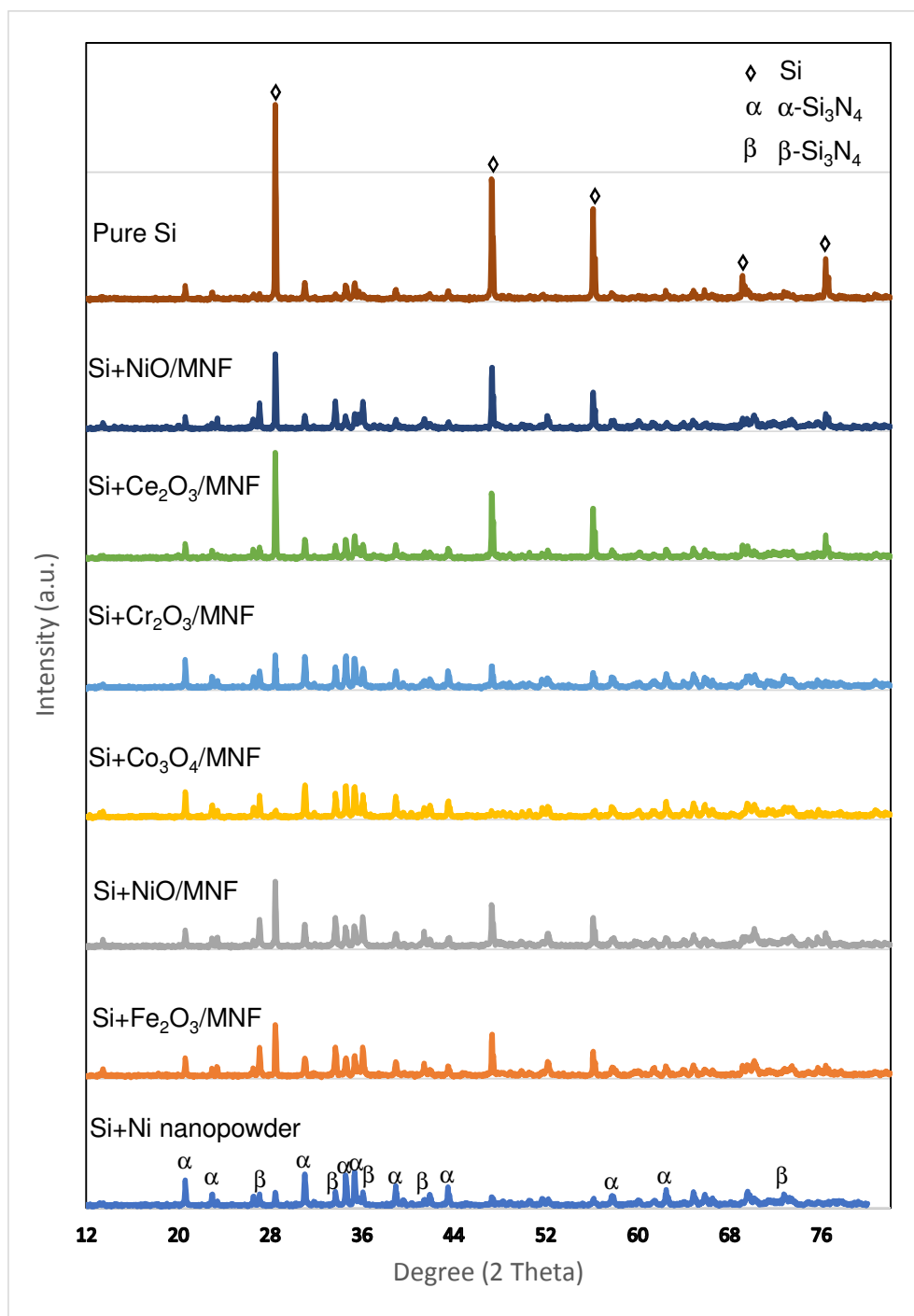


Figure 4.1 XRD patterns of the  $\text{Si}_3\text{N}_4$  network with different catalysts

The direct nitridation of Si powder is regarded as a cost-effective and forthright way for the large-scale production of Si<sub>3</sub>N<sub>4</sub>. However, with this method, noticeable amount of unreacted Si might be remained because of slow reaction process. One strategy to address this issue is use of a suitable catalyst for the Si nitridation process. It is well studied that transition metals/metal oxides contained in silicon as impurities regulate the kinetics of its nitridation [25]. Thus, a higher content of silicon nitride could be achieved by adding a small amount of metals/metal oxides in the raw silicon to promote the nitridation process [25].

The direct nitridation of Si to Si<sub>3</sub>N<sub>4</sub> using various metal and metal oxide as catalysts is studied using die pressing and direct nitridation route. Understanding of the influence of the catalyst on the nitridation degree, as well as the selectivity of the catalyst on the alpha or beta phase formation is the main task of this work.

Figure 4.1 XRD patterns of the samples containing 1.5% catalysts described in the section 3.1.1. Two types of silicon nitrides with different crystal structure were obtained:  $\alpha$ -Si<sub>3</sub>N<sub>4</sub> (trigonal syngony with parameters of a = 7.74 Å, c = 5.61 Å, a:c = 1: 0.725) and  $\beta$ -Si<sub>3</sub>N<sub>4</sub> (hexagonal syngony with parameters of a = 7.604 Å, c = 2.908 Å, a:c = 1: 0.382). It should be noted that Ni nanopowder catalyst leads to formation of most  $\alpha$ -Si<sub>3</sub>N<sub>4</sub>, while when NiO is used mainly  $\beta$ -Si<sub>3</sub>N<sub>4</sub> is obtained with less amount of  $\alpha$ -phase. CeO<sub>2</sub> and Fe<sub>2</sub>O<sub>3</sub> leads to the formation of  $\alpha$ -phase with traces of  $\beta$ -phase. The amount of  $\beta$ -Si<sub>3</sub>N<sub>4</sub> increases using MnO and Co<sub>3</sub>O<sub>4</sub> and Cr<sub>2</sub>O<sub>3</sub>, overall being less than  $\alpha$ -Si<sub>3</sub>N<sub>4</sub>.

Table 4.1 Silicon nitride content of nitridation products

Sample (Si <44 $\mu$ m) +catalyst	Nitrogen content by ONH (%)	Calculated silicon nitride content(%)
Si (without catalyst)	16,97	39,24
MnO/MNF	23,96	55,40
Ce <sub>2</sub> O <sub>3</sub> /MNF	23,11	53,44
Cr <sub>2</sub> O <sub>3</sub> /MNF	33,96	78,53
Co <sub>3</sub> O <sub>4</sub> /MNF	35,31	81,65
NiO/MNF	31,71	73,33
Fe <sub>2</sub> O <sub>3</sub> /MNF	31,64	73,17
Ni (nanopowder)	33.73	84.08

The overall nitridation of silicon samples were studied by ONH analyzer. The results represented in Table 4.1. show that the samples with Co<sub>3</sub>O<sub>4</sub>, Ni nanopowder, are mostly

nitridized, while  $\text{Cr}_2\text{O}_3$ ,  $\text{Fe}_2\text{O}_3$  and provide more or less similar nitridation with 73-78 % nitridation. Taking into account the low nitridation degree of silicon without catalyst, it can be concluded that the catalysts have notable influence on the nitridation. However, cerium oxide and manganese oxide in contrast with other catalysts showed tiny effect, i.e. improve only small amount the nitridation of silicon.

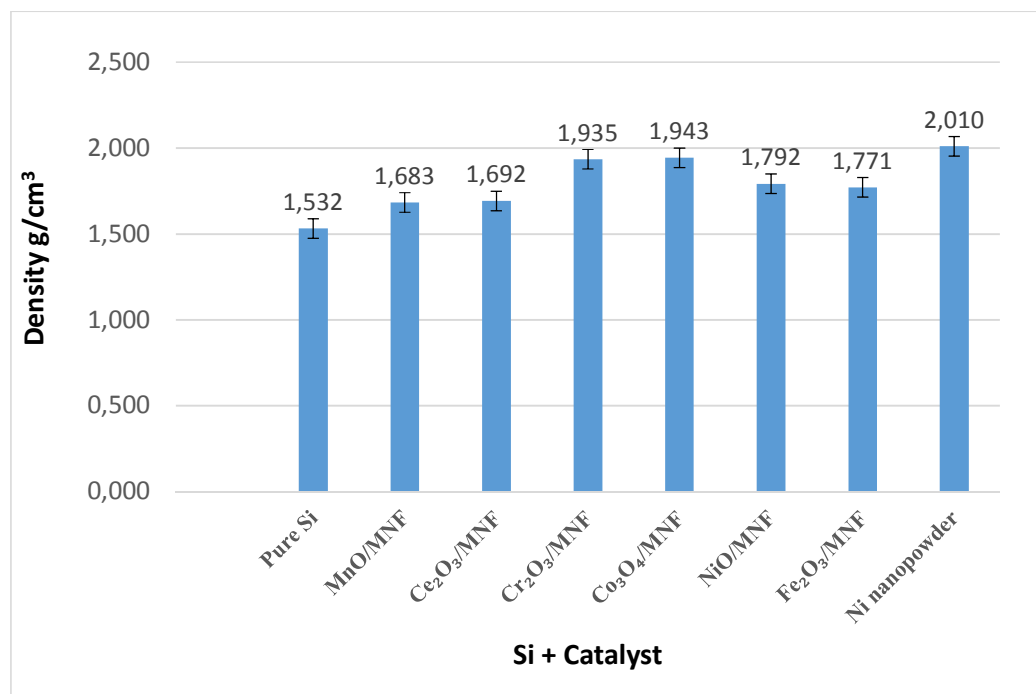


Figure 4.2 Geometric Density of sintered  $\text{Si}_3\text{N}_4$

The density of the samples is proportional to the nitridation degree of silicon (Table 2, Fig. 4.2) almost in all cases. This is caused by the difference of silicon and silicon nitride densities. The samples containing nickel nanopowder,  $\text{Co}_3\text{O}_4/\text{MNF}$  and  $\text{Cr}_2\text{O}_3/\text{MNF}$  show the highest density and is followed by  $\text{NiO}/\text{MNF}$  and  $\text{Fe}_2\text{O}_3/\text{MNF}$ , while silicon shows the lowest density. The densities were kept in the scope of 1.5 to 2.0  $\text{g}/\text{cm}^3$  which is far lower than the fully densified silicon nitride (3.2  $\text{g}/\text{cm}^3$ ).

The overall nitridation is generally increased when metal or metal oxide is added to the silicon raw material. It can be explained by the fact that these metal oxides can be reduced to metals by silicon except  $\text{Ce}_2\text{O}_3$  at the sintering temperature (1300 °C) according to Ellingham-diagram (Fig. 4.3) and these reduced metals are effective in decreasing the melting temperature of the silicon alloy.

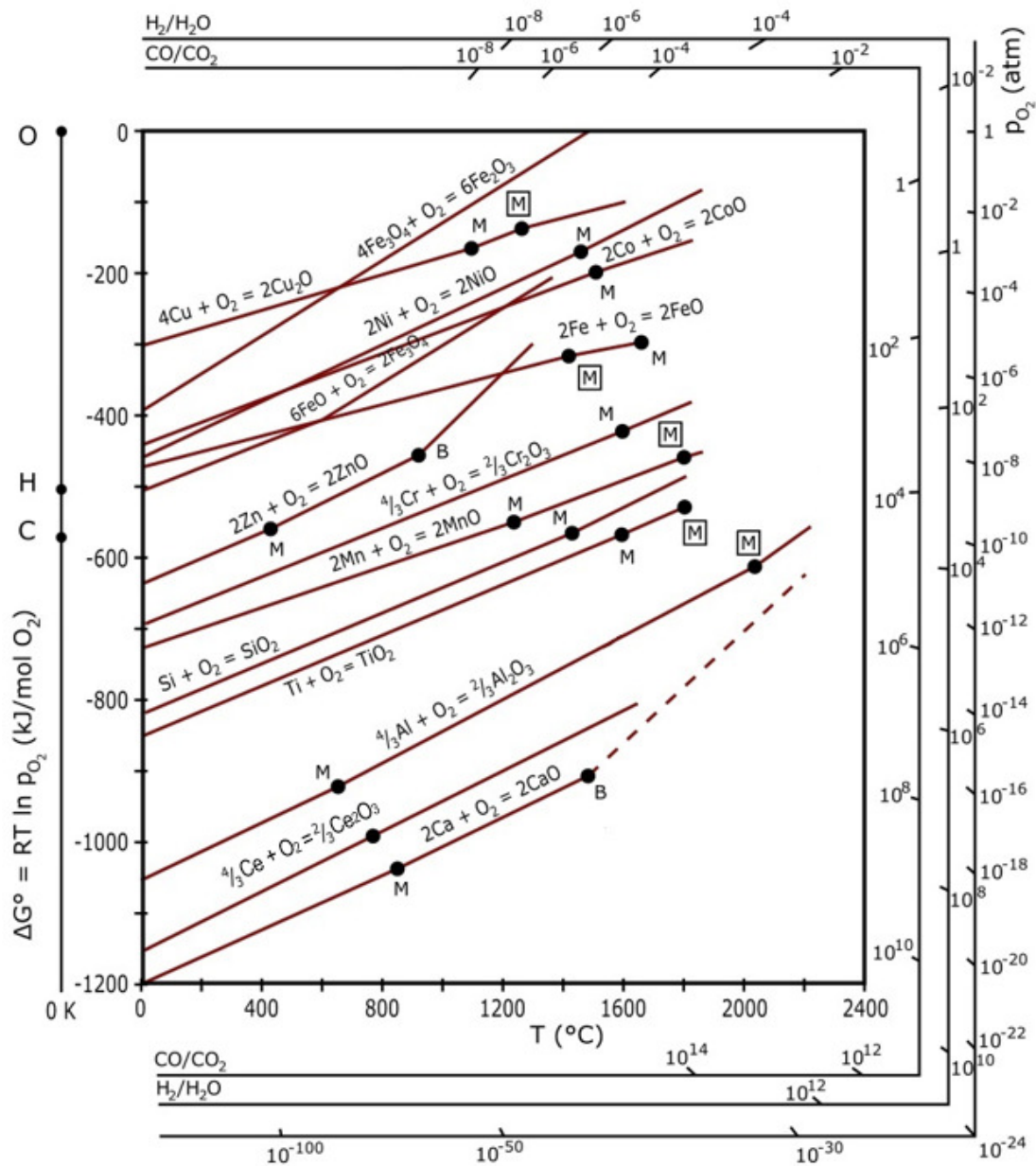


Figure 4.3 Ellingham-diagram [65]

As explained in reference [66], silicon in form of solid, liquid or gas phase can all react with nitrogen to produce silicon nitride. In case of solid reaction,  $3\text{Si(s)} + 2\text{N}_2(\text{g}) = \text{Si}_3\text{N}_4(\text{s})$ , the reaction Gibbs free energy is  $\Delta G = -723 + 0.315T$  kJ/mol. For the reaction of liquid silicon,  $3\text{Si(l)} + 2\text{N}_2(\text{g}) = \text{Si}_3\text{N}_4(\text{s})$  and the Gibbs free energy is  $\Delta G = -874 + 0.405T$  kJ/mol. When it comes to gaseous silicon,  $3\text{Si(g)} + 2\text{N}_2(\text{g}) = \text{Si}_3\text{N}_4(\text{s})$ , the  $\Delta G = -2080 + 0.757T$  kJ/mol. At the current experimental temperature (1573 K), silicon (or silicon alloy) in liquid and gas phase are more easily to react with nitrogen. So, lower melting temperature caused by metal catalyst can promote the nitridation process.

Table 4.2 Melting temperature of silicon and catalyst metals [67]

Element	Melting temperature (°C)
Si	1414
Mn	1246
Ce	795
Cr	1907
Co	1495
Ni	1455
Fe	1538
Ni nanopowder	Less than 1455

The melting temperature of silicon and catalyst metals are shown in Table 4.2. As we know, if one metal contains other metal elements and forms alloy, the melting point will decrease. So, the silicon may be partial melted in the current experimental temperature (1300 °C) and the melted silicon will be nitridized firstly. In case of Ni nanopowder, the real melting temperature will be further lower because of the nanoeffect.

From the nitridation result, manganese has less effect on the nitridation of silicon. The lower melting temperature result in that during the sintering process, the liquid metal just flow away before reaching the reaction starting temperature. The samples "sweat" during the heating and the porosity can be higher.

In case of  $\text{Co}_3\text{O}_4$  there can be additional catalytic effect because of the decomposition reaction of  $\text{Co}_3\text{O}_4$  ( $\text{Co}_3\text{O}_4 \rightarrow 3 \text{CoO} + \frac{1}{2} \text{O}_2$ ) at 600-700°C, which leads to the formation of CoO [68]. This reaction may enlarge the porosity of the material and be beneficial for the penetration of nitrogen.

In order to illustrate the role of catalyst in the morphology of nitridized samples, it was investigated the microstructure fracture of the samples. Figure 4.4 shows that  $\text{Si}_3\text{N}_4$  nanofibers grown during the nitridation has 300-400nm diameter. It can be seen that samples containing no catalyst and containing  $\text{Ce}_2\text{O}_3$  or MnO possess less fibers, while  $\text{Co}_3\text{O}_4$ , NiO,  $\text{Fe}_2\text{O}_3$  and Ni nanopowder promote formation of fibrous silicon nitride. Ni and NiO catalyst generate more straight fibers. The fibers were abundant and they intertwined together as network. The formation process of the  $\text{Si}_3\text{N}_4$  fibers could be governed by the vapor-liquid-solid growth mechanism or a solid-liquid-gas-solid growth mechanism as explained in reference [43].

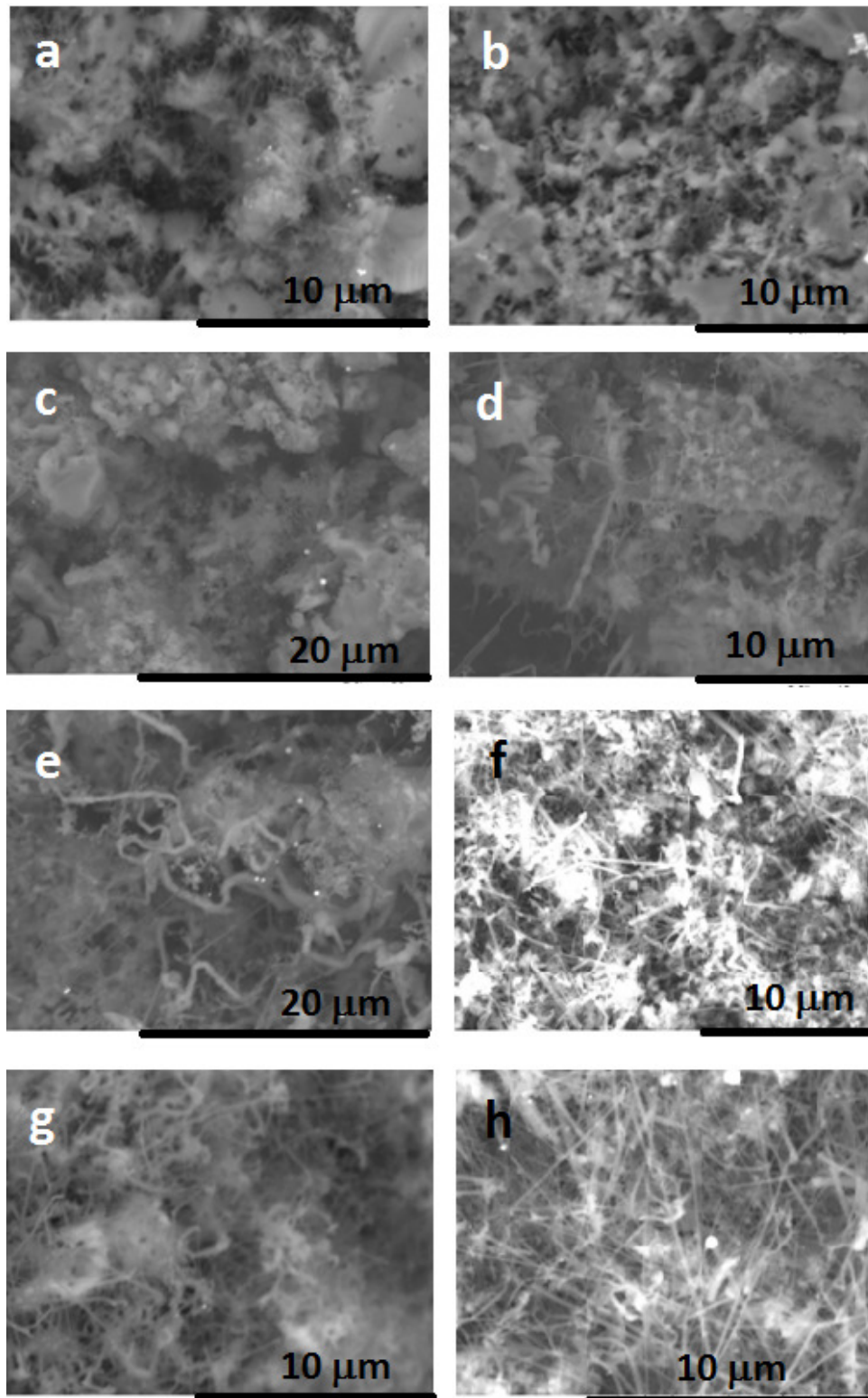


Figure 4.4. SEM images of silicon samples after heat treated in  $N_2$  at  $1300\text{ }^\circ\text{C}$  for 5 hours containing (a) no catalyst, (b)  $MnO/MNF$ , (c)  $Ce_2O_3/MNF$ , (d)  $Cr_2O_3/MNF$ , (e)  $Co_3O_4/MNF$ , (f)  $NiO/MNF$ , (g)  $Fe_2O_3/MNF$ , (h)  $Ni$  nanopowder.

#### 4.1.2 Influence of the nitridation atmosphere

The nitridation of silicon is carried out also in ammonia diluted in nitrogen atmosphere. It is proposed that ammonia can enhance the nitridation of silicon as it has reducing nature and can reduce adsorbed oxygen on the silicon powder, as well as, reduce the oxide catalysts into metals.

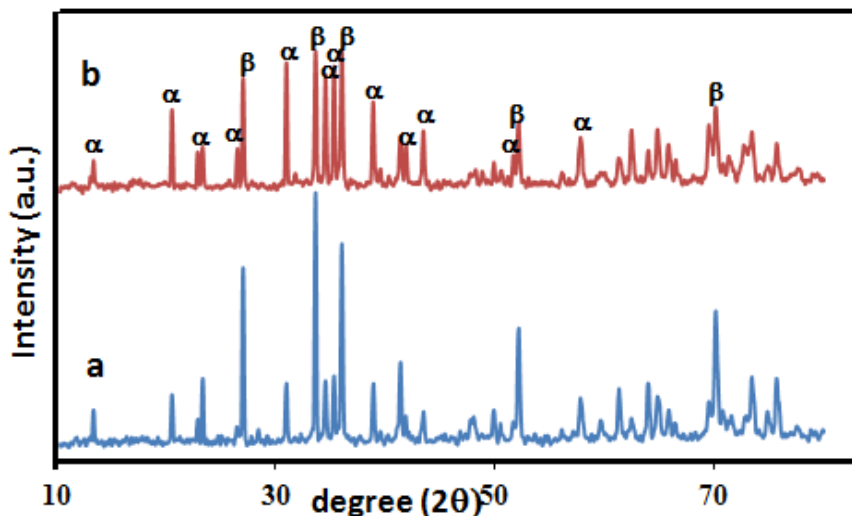


Figure 4.5. XRD patterns of samples containing NiO/MNF catalyst after nitridation at (a) nitrogen, (b) 10vol.%NH<sub>3</sub> diluted in nitrogen atmosphere.

Figure 4.5 illustrates the XRD pattern of the samples containing NiO catalyst after heat treatment at N<sub>2</sub> and NH<sub>3</sub> diluted in nitrogen atmosphere. At nitrogen atmosphere mainly β-Si<sub>3</sub>N<sub>4</sub> is obtained with some traces of α-phase. While at ammonia atmosphere the peaks related to α-Si<sub>3</sub>N<sub>4</sub> increases intensively.

The Figure 4.6 picturizes the morphology of the nitridized samples. The sample containing no catalyst possess agglomerated structure, while samples containing catalysts are fibrous. It should be noted that MnO containing sample is the less fibrous sample after the sample without catalyst. It can be concluded that the samples treated in ammonia atmosphere have similar morphology as the sample treated in nitrogen, except Ce<sub>2</sub>O<sub>3</sub> containing sample, which becomes fibrous when heated at ammonia atmosphere.

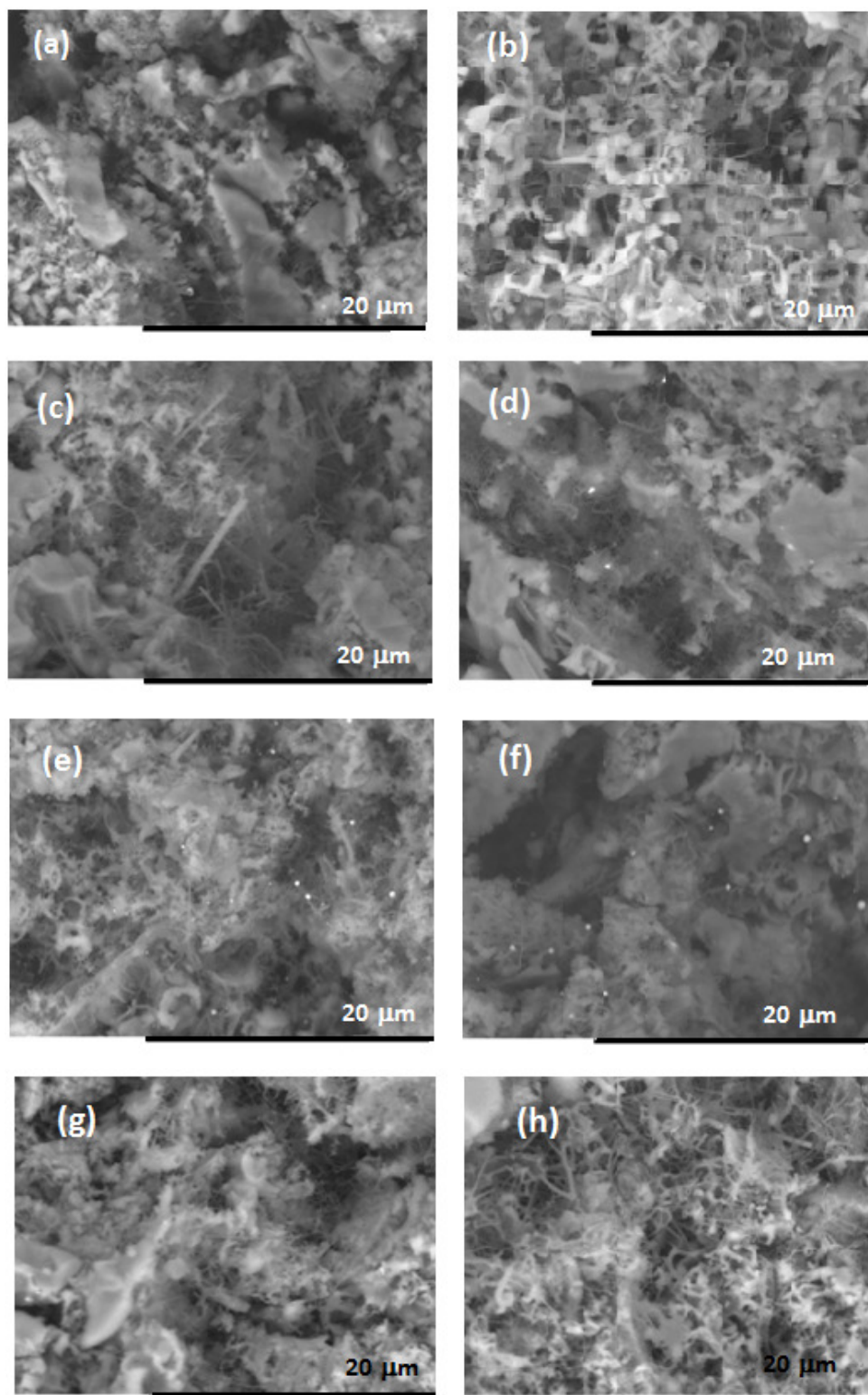


Figure 4.6. SEM images of silicon samples after heat treated in  $\text{NH}_3$  diluted in nitrogen at  $1300\text{ }^\circ\text{C}$  for 5 hours containing (a) no catalyst, (b)  $\text{MnO/MNF}$ , (c)  $\text{Ce}_2\text{O}_3/\text{MNF}$ , (d)  $\text{Cr}_2\text{O}_3/\text{MNF}$ , (e)  $\text{Co}_3\text{O}_4/\text{MNF}$ , (f)  $\text{NiO/MNF}$ , (g)  $\text{Fe}_2\text{O}_3/\text{MNF}$ , (h)  $\text{Ni}$  nanopowder.

## 4.2 Fibrous silicon nitride network with complex geometry

After investigating the catalytic effect of the chosen catalysts on the nitridation of silicon, a manufacturing process to obtain complex shaped silicon nitride based components are designed.

### 4.2.1. Selective laser sintering of silicon

The process consists of two main processes; (i) selective laser sintering of silicon component, and (ii) nitridation of components. Selective laser sintering was performed both in argon and nitrogen environment. The nitrogen and oxygen content (considering that the admissible limit of the oxygen in gaseous environment is 0.5 vol.%) in the shaped samples was checked by XRD. According to the diffraction patterns (Fig 4.7) no nitridation or oxidation of silicon took place during SLS process (both oxygen and nitrogen level was below 500ppm).

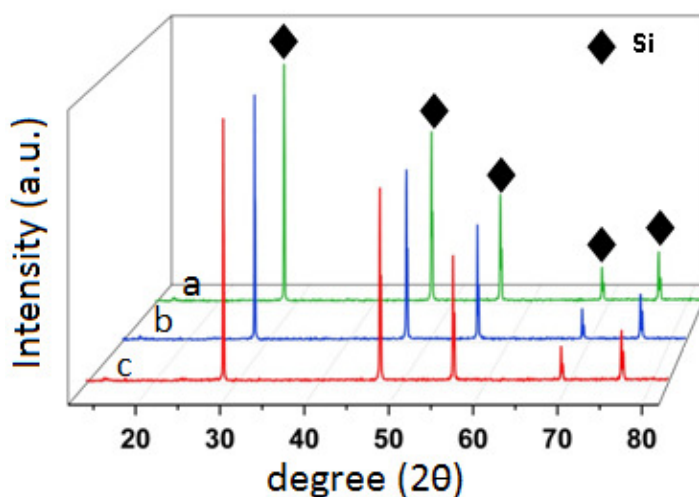


Figure 4.7 XRD patterns of silicon sintered in (a) Ar, using 1100mA, (b) in Ar, using 500mA and (c) in N<sub>2</sub>, using 500 mA laser current

As explained in 3.1.3, there are 3 main parameters effecting the SLS process: laser current, point distance and exposure time. Our first task was to find out the best parameter for this sintering process. For the 18 cubic samples produced by SLS with exposure time from 125-375  $\mu$ s, point distance from 10-30  $\mu$ m and laser current 500 and 1100 mA (Table 3.3), Geometric density and Archimedes density were measured firstly (Table 4.3).

For the selective laser sintering of silicon, the layer thickness was chosen as 25 $\mu$ m. The laser current, point distance and exposure time were altered in 500-1100 mA, 125-375 $\mu$ s and 10-30 $\mu$ m range respectively. It was studied that exposure time and point distance don't influence significantly on sintering behavior and morphology of silicon, while laser current has

a key role on the morphology of the sintered powder. The cubes sintered with higher laser current have higher geometric density, compared to the others obtained by using low laser current. While the Archimedes density is about the same for all produced shapes. The latter led us to conclude that increasing the laser current makes the samples less porous. The next step of our investigation was to find out the optimum laser current for the sintering process. For this purpose, the laser current was changed in 400-1300 mA range, while keeping proposed 10  $\mu\text{m}$  point distance and 125  $\mu\text{s}$  exposure time.

*Table 4.3 Densities and relative densities of SLS processed silicon samples*

<b>Sample</b>	<b>Exposure time(<math>\mu\text{s}</math>)</b>	<b>Point distance (<math>\mu\text{m}</math>)</b>	<b>Laser current (mA)</b>	<b>Density-Geom. (<math>\text{g}/\text{cm}^3</math>)</b>	<b>Geom. Relative density (%)</b>	<b>Density-Arch. (<math>\text{g}/\text{cm}^3</math>)</b>	<b>Arch. Relative density (%)</b>
1	125	10	500	1.46	62.68	2.25	96.60
2	125	20	500	1.36	58.39	2.32	99.61
3	125	30	500	1.21	51.95	2.20	94.46
4	250	10	500	1.48	63.54	2.32	99.61
5	250	20	500	1.41	60.54	2.21	94.89
6	250	30	500	1.29	55.38	2.24	96.17
7	375	10	500	1.54	66.12	2.32	99.61
8	375	20	500	1.53	65.69	2.31	99.18
9	375	30	500	1.45	62.25	2.25	96.60
10	125	10	1100	1.78	76.72	2.33	100.4
11	125	20	1100	1.64	70.69	2.23	96.12
12	125	30	1100	1.67	71.98	2.21	95.26
13	250	10	1100	1.80	77.59	2.24	95.55
14	250	20	1100	1.83	78.88	2.30	99.14
15	250	30	1100	1.72	74.14	2.21	95.26
16	375	10	1100	1.92	82.76	2.29	98.71
17	375	20	1100	1.99	85.78	2.25	96.98
18	375	30	1100	1.82	78.45	2.19	94.40

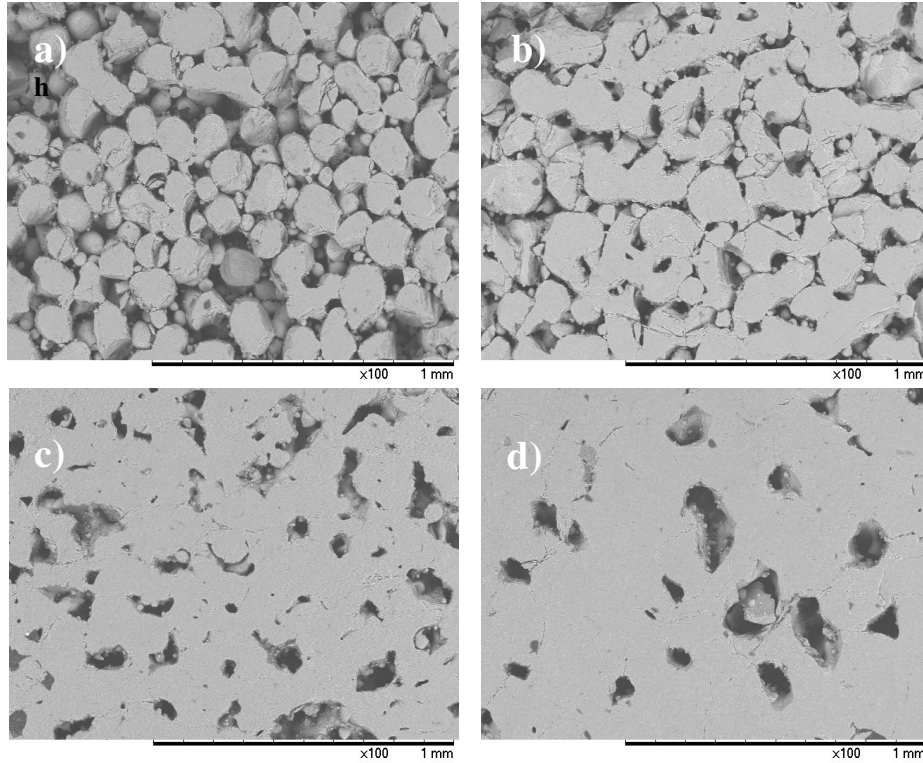


*Figure 4.8 SEM images of silicon samples produced by SLS using a)500, b)700, c)900 and d)1100 mA laser currents*

According to the microstructure of produced parts (Fig. 4.8) it is obvious that the samples printed by 500 and 700 mA laser current were much more porous and brittle, whereas SLS processed parts by supplying higher laser current were denser and stronger. Using the less than 500 mA laser current doesn't lead the complete shape formation of samples, while the samples printed with higher laser current as 1100 mA, the printed layer could be remelted and removed by the wiper which result in the failure of the process.

As a result, 900 mA laser current, 10  $\mu\text{m}$  point distance and 125  $\mu\text{s}$  exposure time were chosen as the optimized parameter for further experiments.

#### **4.2.2 Nitridation of shaped silicon samples**

$\text{Co}_2\text{O}_3/\text{MNFs}$  were mixed with the silicon powder and 3D printed by SLS with optimized parameters (900 mA laser current, 10  $\mu\text{m}$  point distance and 125  $\mu\text{s}$  exposure time). The sample was further nitridized as described in section 3.1.2. From the XRD pattern (Fig. 4.9), some of silicon was nitridized. Compare with die pressed samples, it is less homogeneous because during the laser sintering process, some of the silicon powders were melted and agglomerated together

(Fig. 4.10). The fibrous network can be observed in the gaps between agglomerated silicon parts.

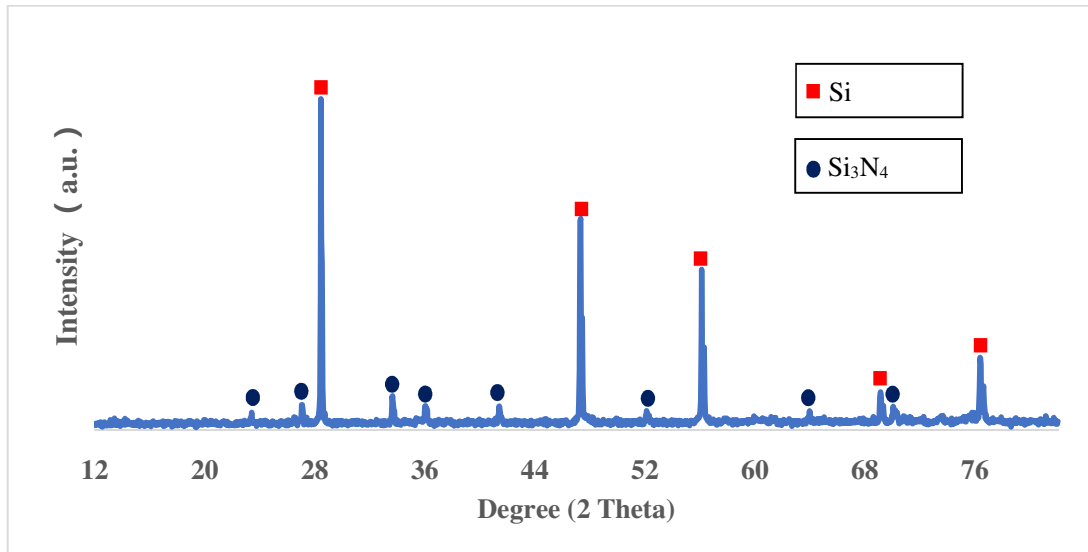


Figure 4.9 XRD pattern of Si<sub>3</sub>N<sub>4</sub> sample made by SLS and nitridation (catalyst Co<sub>3</sub>O<sub>4</sub>/MNF)

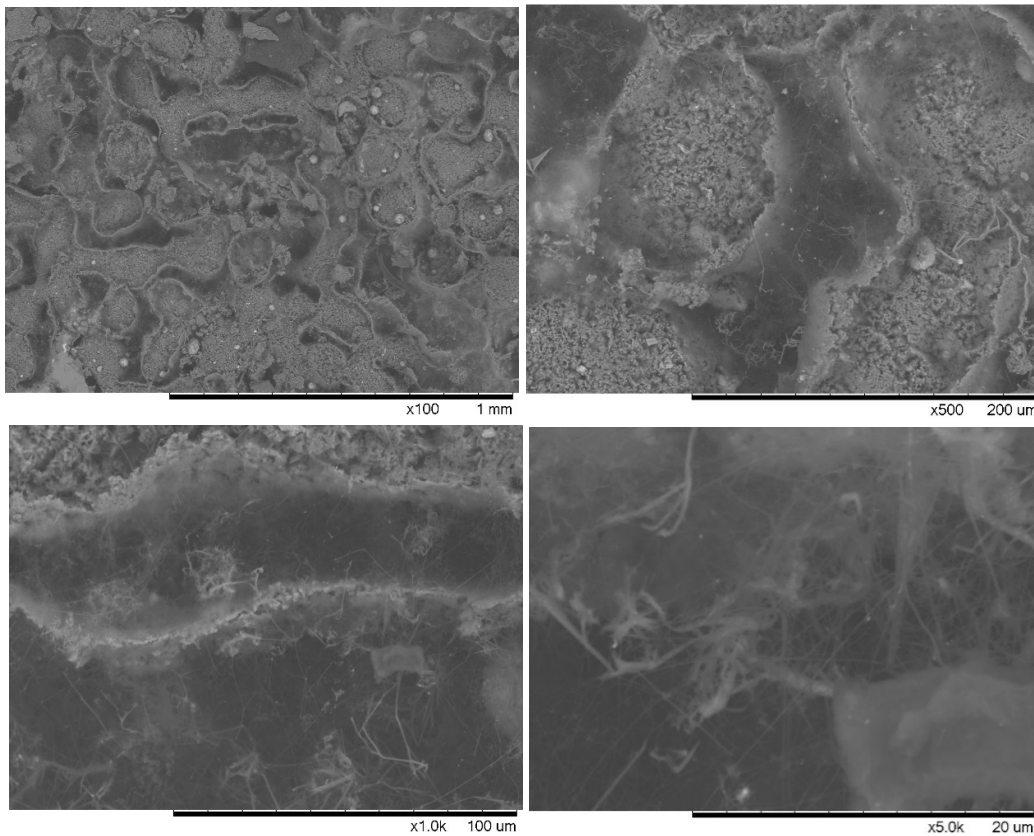


Figure 4.10 SEM image of Si<sub>3</sub>N<sub>4</sub> sample made by SLS and nitridation (catalyst Co<sub>3</sub>O<sub>4</sub>/MNF)

### 4.3 Mechanical properties and thermal stability of fibrous Si<sub>3</sub>N<sub>4</sub> network

#### 4.3.1 Mechanical properties of Si<sub>3</sub>N<sub>4</sub> network

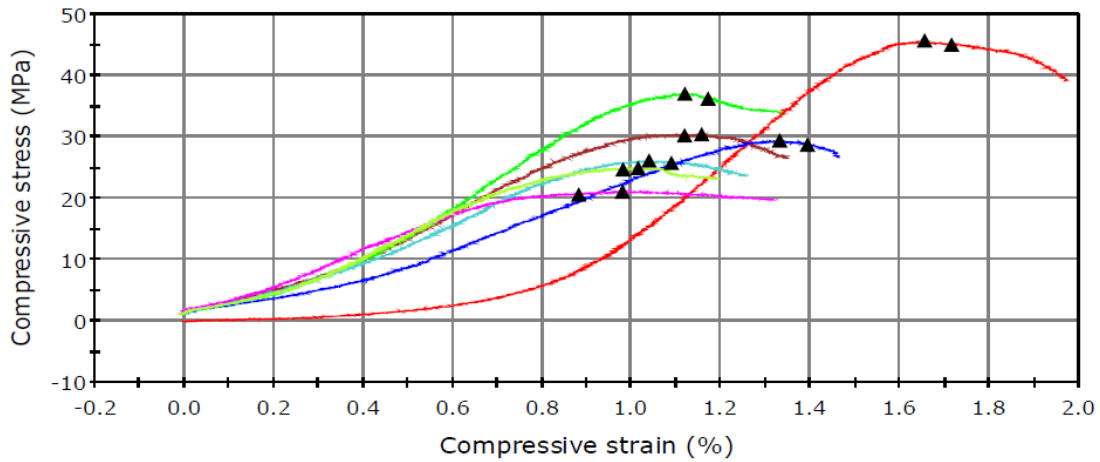


Figure 4.11 Compressive stress-strain curve of Si<sub>3</sub>N<sub>4</sub> network (NiO/MNF as catalyst)

Table 4.4 Compression test result of Si<sub>3</sub>N<sub>4</sub> network (NiO/MNF as catalyst)

	Specimen label	Rate 1 (mm/min)	Compressive max stress (MPa)	Yield (Slope Threshold 0,2 %) (MPa)	max Compressive ext (mm)	Maximum Load (kN)	Modulus (Automatic) (GPa)	Anvil height (mm)	Diameter (mm)
1	1	0,127	45,7	45,0	0,498	5,50	6,32	30,100	12,38
2	2	0,127	30,4	30,3	0,339	3,71	4,05	29,300	12,47
3	3	0,127	37,0	36,2	0,330	4,47	4,85	29,470	12,39
4	4	0,127	26,1	25,8	0,302	3,20	3,47	29,060	12,48
5	5	0,127	29,4	28,7	0,393	3,58	2,92	29,550	12,45
6	6	0,127	21,2	20,6	0,287	2,58	3,21	29,320	12,46
7	7	0,127	25,0	24,7	0,292	3,02	3,80	28,760	12,40
Mean		0,127	30,7	30,2	0,349	3,72	4,09	29,366	12,43
Standard Deviation		0,00000	8,28089	8,14791	0,07515	0,98443	1,16690	0,41848	0,04152

The mechanical properties of Si<sub>3</sub>N<sub>4</sub> network was measured by compression test. The specimen was prepared by die pressing and direct nitridation route with NiO/MNF as catalyst. Fig. 4.11 illustrates the stress-strain curves of seven specimens. As calculated in Table 4.4, the highest compressive strength can reach 45.0 MPa. The average compressive strength was 30.7 MPa and the average yield strength was 30.2 MPa.

### 4.3.2 Thermal stability of Si<sub>3</sub>N<sub>4</sub> network

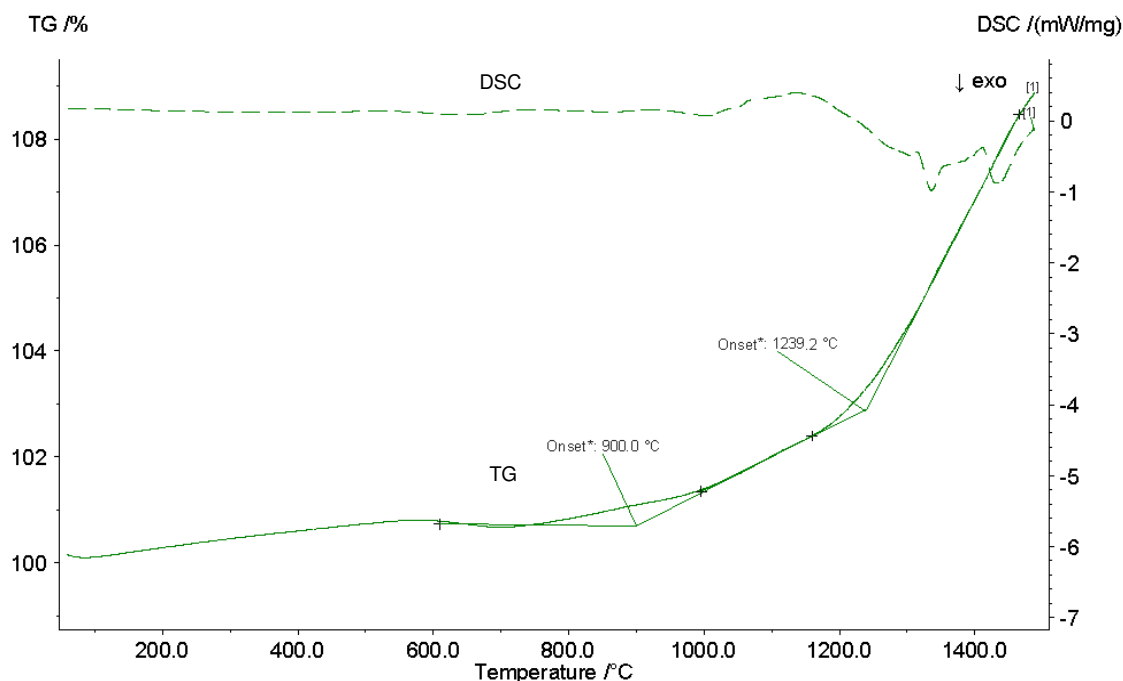


Figure 4.12 DSC/TG curve of Si<sub>3</sub>N<sub>4</sub> network

Thermal stability of Si<sub>3</sub>N<sub>4</sub> network can be analyzed from DSC/TG curve (Fig. 4.12). The specimen was also prepared by die pressing and direct nitridation with Co<sub>3</sub>O<sub>4</sub>/MNF as catalyst. For this fibrous Si<sub>3</sub>N<sub>4</sub> network, there is practically no strong DSC signals until 1000°C, despite small mass gains already seen from 700-900°C. The most intensive mass gain (TG) accelerates over 1200°C yet with complex and moderate exothermic effects. Theoretically, the reaction is  $\text{Si}_3\text{N}_4 + 3\text{O}_2 = 3\text{SiO}_2 + 2\text{N}_2$ , which for 1 mg of fully oxidized nitride would give about  $3 \cdot 60 / 140 = 1.286$  mg silicon dioxide, i.e. ~28% increase. If this would be the case, ~9% weight gain would mean ~30% of oxidized material.

## 4.4 Si<sub>3</sub>N<sub>4</sub> fiber

### 4.4.1 Morphology of Si<sub>3</sub>N<sub>4</sub> fiber

During the nitridation of silicon containing NiO, Fe<sub>2</sub>O<sub>3</sub>, Co<sub>3</sub>O<sub>4</sub> or Ni nanopowder catalysts, the Si<sub>3</sub>N<sub>4</sub> fibers in diameter of 300nm-2µm were grown also on the lips of the graphite crucible. It was further found that, nickel nanopowders stimulates the formation of silicon nitride fibers more intensively than others (Fig. 4.13). The metallic droplets distinguished on each terminal of the fibers shows that the fibers were grown based on VLS mechanism as

explained in reference [43]. This is a simple way of producing silicon nitride fibers and can be easily scale up.

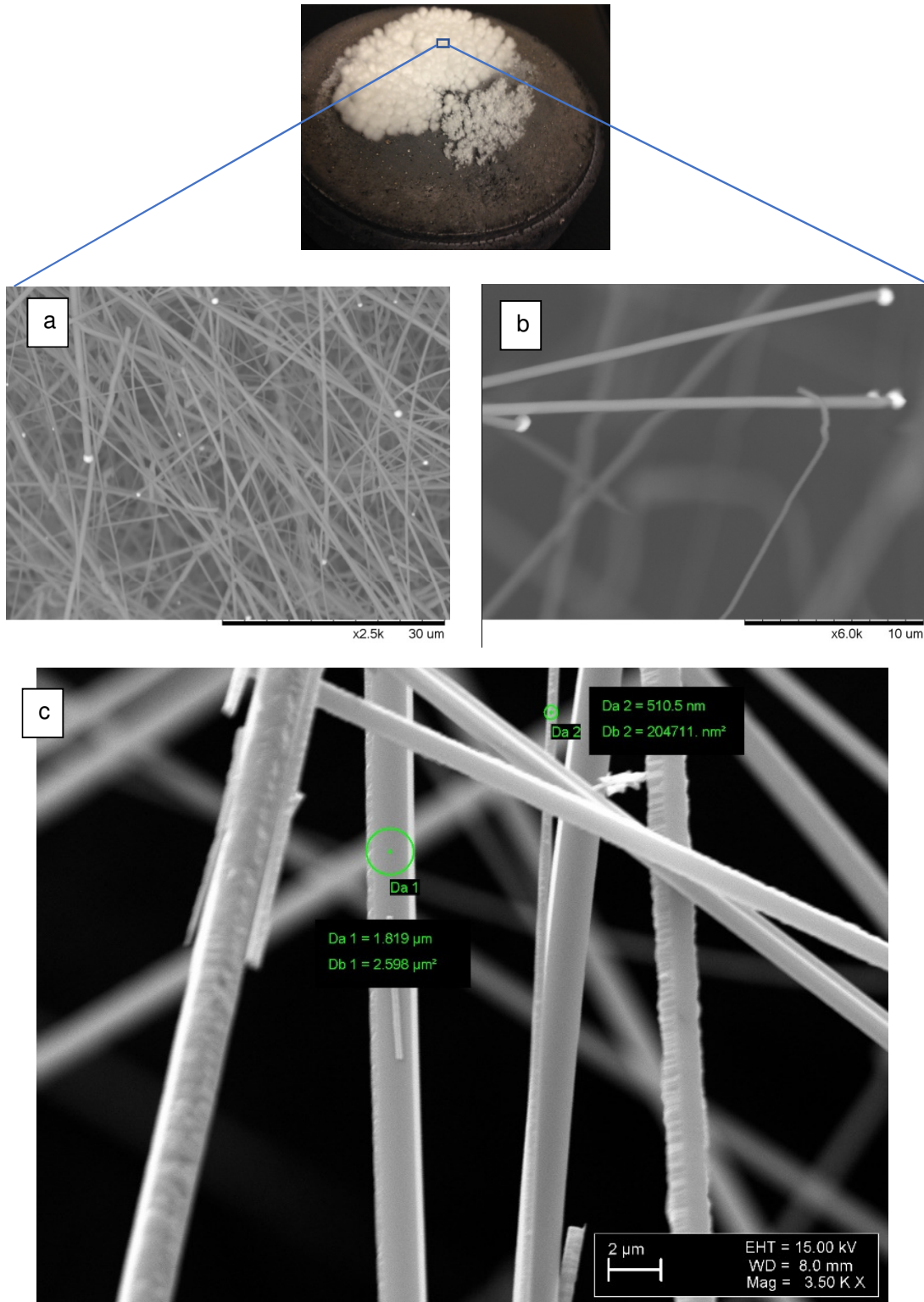


Figure 4.13  $\text{Si}_3\text{N}_4$  fibers grown from crucible lips (Ni nanopowders as catalyst)  
a) Fibers with irregular directions b) Fibers with droplets c) Diameter of fibers

#### 4.4.2 Composition of Si<sub>3</sub>N<sub>4</sub> fiber

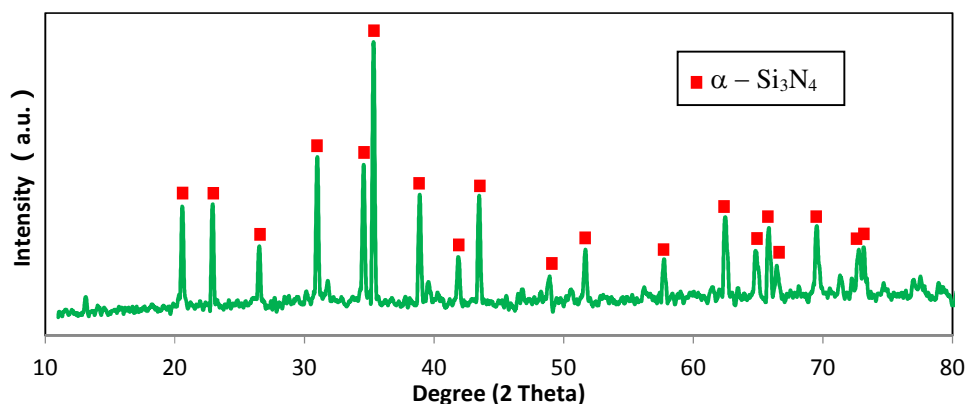


Figure 4.14 XRD pattern of Si<sub>3</sub>N<sub>4</sub> fibers ( Ni nanopowders as catalyst)

A piece of silicon nitride fibers collected from was pressed as layer type and analyzed by XRD. From the XRD result (Fig. 4.14), it was shown that the fibers were composed of only pure  $\alpha$ -Si<sub>3</sub>N<sub>4</sub>. All the peaks were sharp and clear, which means the purity of obtained silicon fibers were high.

#### 4.4.3 Thermal stability of Si<sub>3</sub>N<sub>4</sub> fiber

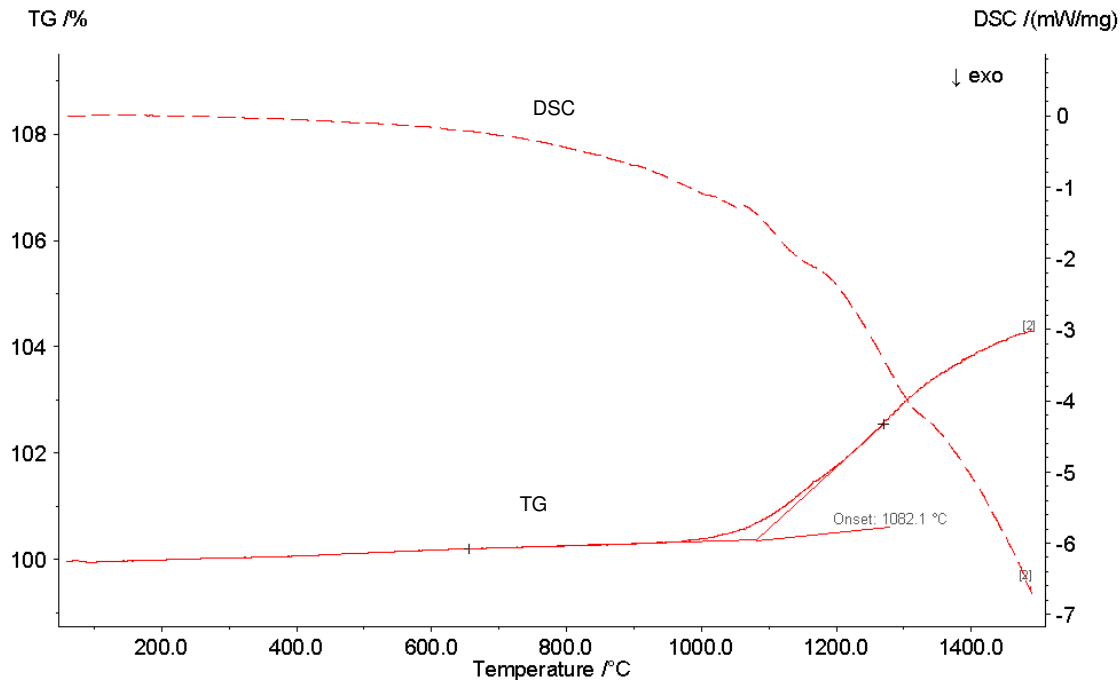


Figure 4.15 DSC/TG analysis of Si<sub>3</sub>N<sub>4</sub> fibers

Ceramic fibers get most of their applications at high temperature, so the thermal stability of these fibers is important. The same as Si<sub>3</sub>N<sub>4</sub> network, Si<sub>3</sub>N<sub>4</sub> fibers were also analyzed by

DSC/TG (Fig. 4.15). For  $\text{Si}_3\text{N}_4$  fibers, it started to be oxidized over  $1000^\circ\text{C}$  (TG curve), although small weight gain is seen already at lower temperatures. This is supported by DSC signal turning into exothermic side already after  $600^\circ\text{C}$  and continuously increasing. Total mass gain is about 4%, so about 0.15 fraction of all fibers were converted into silica. The layer of  $\text{SiO}_2$  may work as a protective layer preventing further oxidation at  $600\text{-}1000^\circ\text{C}$ .

## CONCLUSIONS

In this work, the fibrous silicon nitride networks of multi-axis architecture were prepared by two-steps route including production of the precursor shape of the required network of silicon by a die pressing or a SLS, and subsequent direct nitridation to produce the fibrous network of silicon nitride. The nitridation was carried at the pressure-less furnace at 1300 °C for 5 hours. The effect of several catalysts on process of nitridation and properties of the final products were thoroughly studied. From these studies the following conclusions can be made:

1. The fibrous silicon nitride network of multi-axis architecture was successfully synthesized with the help of both the selective laser technique and die pressing.
2. The  $\text{Co}_3\text{O}_4/\text{MNF}$ ,  $\text{Cr}_2\text{O}_3/\text{MNF}$ ,  $\text{NiO}/\text{MNF}$  and  $\text{Fe}_2\text{O}_3/\text{MNF}$  prepared by the solution combustion method were found to be the suitable catalysts for the nitridation of silicon.
3. The sintering parameters of SLS were optimized in terms of exposure time, point distance and laser current of treatment. The complex-shaped substrate materials were obtained for further treatment.
4. The obtained silicon nitride networks have the specific properties:
  - a. Self-reinforcement by the in-site growth of the silicon nitride fibers. The compressive strength can reach up to 45 MPa.
  - b. Stability during heating in air until 700 °C.
5. The silicon nitride fibers can grow during the nitridation process:
  - a. A simple and easily scale up method of producing pure  $\alpha\text{-Si}_3\text{N}_4$  fibers has been developed.
  - b. The  $\text{Si}_3\text{N}_4$  fibers are stable below 1000 °C in the air conditions.

Currently, although fibrous  $\text{Si}_3\text{N}_4$  network and  $\text{Si}_3\text{N}_4$  fibers can be successfully produced, there are still large amount of work needs to be done in the future. For example, scaling up the process for the industrial production; testing the biocompatibility for possible application as bio-scaffold; further functionalization of the material to improve the electrical conductivity, etc.

## RÉSUMÉ

Silicon nitride ( $\text{Si}_3\text{N}_4$ ) as one of widely used ceramic material has found its main applications in a variety of areas, such as heat exchanger bearings, chemical reaction vessels, high-temperature components, automotive and aerospace parts due to good thermal performance, mechanical strength, biocompatibility and chemical stability. The fibrous morphology of the  $\text{Si}_3\text{N}_4$  substrates are highly desirable for specific applications, e.g. bio-scaffolds, heat sinks, etc. However, their manufacturing is faced with a number of problems, such as a large-scale synthesis of fibers in a cost-effective way, their incorporation and homogeneous distribution throughout a matrix material, their potential hazard arising from asbestos-like fibers.

Additive manufacturing is gaining increasing attention as it provides the cost-effective and waste-less production route for the materials of complex multi-axis geometries. The sintering of ceramic-based materials is still under intensive study and represents the specific challenge for researchers. There is very limited number of works related to the additive manufacturing of the silicon nitride.

This thesis aims at designing a high-tech manufacturing methodology, which will enable facile production of fibrous networks of  $\text{Si}_3\text{N}_4$  with sophisticated geometry. The fibrous network has been processed by two-step production routine: (i) a die pressing or a selective laser sintering of pure silicon to get a net-shape silicon tracery; and (ii) nitridation of the silicon precursor network to turn it into the fibrous silicon nitride network. The catalysts of NiO,  $\text{Ce}_2\text{O}_3$ ,  $\text{Fe}_2\text{O}_3$ , MnO,  $\text{Cr}_2\text{O}_3$  and  $\text{Co}_3\text{O}_4$  carried by novel mullite nanofibers (MNF) substrate were chosen for this study. Commercial Ni nanopowder was used as reference. The catalytic effect of catalysts on the nitridation process of silicon was thoroughly studied. The morphology and properties of the final products were comprehensively studied with the help of SEM, XRD, DSC/TG and ONH analyzer. It was found that the catalyst plays a key role for the process of nitridation.

The breakthrough lies in the development of manufacturing process to fabricate innovative multi-axis materials with special properties via the smart manufacturing technology-selective laser sintering including preparation of the porous silicon network by 3D printing, simultaneous nitridation and growth of the silicon nitride fibers from the precursor network.

## RESÜMEE

Räninitriid ( $\text{Si}_3\text{N}_4$ ) on laialdaselt kasutatud keraamiline materjal, mida kasutatakse mitmesugustes valdkondades nagu näiteks soojusvahetite laagrid, keemias kasutatavad reaktsioonianumad, kõrge temperatuuriga komponendid, autoosad ja lennundus. Lisaks sobib  $\text{Si}_3\text{N}_4$  komponentide kiuline morfoloogia hästi mitmesugustes rakendustes (nt. biotoesed, soojusvahetid jm.) kasutamiseks, kuna neil on hea soojuskasutus, mehaaniline tugevus, täiustatud bioühilduvus jne. Kuid nende tootmisel esineb mitmesuguseid probleeme nagu näiteks kiudude efektiivne suuremahuline sünteesimine, nende difusioon ja maatriksisse sidumine, potentsiaalsed asbestkiududega seotud ohud jms.

3D printimine kogub ühe rohkem tähelepanu, kuna see võimaldab mitmeteljelise geomeetriaga materjalide tasuvat ja jäätmeteta tootmist. Keerulise kujuga materjale kasutatakse laialdaselt paljudes tööstuslikes rakendustes. Kuid räninitriidi 3D printimist kasutatakse praegu veel vähe.

Käesoleva töö eesmärk on kujundada kõrgtehnoloogiline tootmismetoodika, mis võimaldab keerulise geomeetriaga  $\text{Si}_3\text{N}_4$  kiudvõrkude hõlpsat tootmist. Sellise võrgu valmistamiseks pakutakse välja 2-etapiline tootmisprotsess: (i) räni valupressimine või selektiivne laserpaagutus võrgukujulise ränivõre saamiseks, (ii) ränivõrgu nitriitimine kiudja räninitriidivõrgu saamiseks. Katalüsaatoriteks valiti uudse mulliit-nanokiuga (MNF) seotud  $\text{NiO}$ ,  $\text{Ce}_2\text{O}_3$ ,  $\text{Fe}_2\text{O}_3$ ,  $\text{MnO}$ ,  $\text{Cr}_2\text{O}_3$  ja  $\text{Co}_3\text{O}_4$ . Võrdluseks valiti ka kaubanduslikult saadav Ni nanopulber. Uuriti nimetatud katalüsaatorite katalüütilist mõju räni nitriitimise protsessile. Toode morfoloogiat ja omadusi uuriti põhjalikult SEM, XRD, DSC/TG ja ONH analüsaatoritega. Leiti, et nendel katalüsaatoritel on oluline roll nitriitimise protsessis.

Läbimurre seisneb tootmisprotsessi edasiarenduses, mis võimaldab luua uuenduslikke eriomadustega mitmeteljelisi materjale, kasutades selleks arukat tootmistehnoloogiat - selektiivset laserpaagutust, sealhulgas poorse ränivõrgu 3D printimist, samaaegset nitriitimist ja võrgust kiudude kasvatamist.

## REFERENCE

- [1] Sangster, Raymond C. "FORMATION OF SILICON NITRIDE: FROM THE 19<sup>th</sup> TO THE 21<sup>st</sup> CENTURY." *Materials Science Foundations* (2005): 948.
- [2] Tsuge Akihiko, K. Nishida, and M. Komatsu. "Effect of Crystallizing the Grain-Boundary Glass Phase on the High-Temperature Strength of Hot-Pressed Si<sub>3</sub>N<sub>4</sub> Containing Y<sub>2</sub>O<sub>3</sub>." *Journal of the American Ceramic Society* 58, no. 7-8 (1975): 323-326.
- [3] Yoshio UK, Shigetaka WA. High strength Si<sub>3</sub>N<sub>4</sub> ceramics. *Journal of the Ceramic Society of Japan*. 1989 Aug 1;97(1128):872-4.
- [4] T.J. Webster, A.A. Patel, M.N. Rahaman, and B.S. Bal, "Anti-Infective and Osteointegration Properties of Silicon Nitride, Poly (Ether Ether Ketone), and Titanium Implants," *Acta Biomater.*, 8 [12] 4447–4454 (2012).
- [5] Lange Horst, Gerhard Wötting, and Gerhard Winter. "Silicon nitride—from powder synthesis to ceramic materials." *Angewandte Chemie International Edition in English* 30.12 (1991): 1579-1597.
- [6] Mc Entire BJ et al. (2016) Processing and Characterization of Silicon Nitride Bioceramics. *Bioceram Dev Appl* 6:093. doi:10.4172/2090-5025.1000093
- [7] Taylor R. M., J. P. Bernero, A. A. Patel, D. S. Brodke, and A. C. Khandkar. "Silicon nitride: a new material for spinal implants." In *Orthopaedic Proceedings*, vol. 92, no. SUPP I, pp. 133-133. *Orthopaedic Proceedings*, 2010.
- [8] Amedica, US Spine Enters the reconstructive surgery market: first silicon nitride total hip replacement. 2011 [Published: 17 Feb 2011, Accessed: 6 Aug 2013].[http://www.amediacorp.com/press\\_releases/amedica\\_us\\_spine\\_enters\\_the\\_reconstructive\\_surgery\\_market](http://www.amediacorp.com/press_releases/amedica_us_spine_enters_the_reconstructive_surgery_market)
- [9] Kannan G B, Rajendran D K. A Review on Status of Research in Metal Additive Manufacturing, *Advances in 3D Printing & Additive Manufacturing Technologies*. Springer Singapore, 2017: 95-100.
- [10] Kitayama M., K. Hirao, M. Toriyama, and S. Kanzaki. "Modeling and simulation of grain growth in Si<sub>3</sub>N<sub>4</sub>-Anisotropic Ostwald ripening." *Acta materialia* 46, no. 18 (1998): 6541-6550.
- [11] Jiang J. Z., Flemming Kragh, D. J. Frost, and H. Lindelov. "Hardness and thermal stability of cubic silicon nitride." *Journal of Physics: Condensed Matter* 13, no. 22 (2001): L515.
- [12] Riley Frank L. Silicon Nitride and Related Materials. *Journal of the American Ceramic Society*. 2004, 83 (2): 245-265.
- [13] Hong Peng. Spark Plasma Sintering of Si<sub>3</sub>N<sub>4</sub>-Based Ceramics, (PhD thesis). Stockholm University. (2004)

- [14] Carter C. Barry & Norton M. Grant (2007). *Ceramic Materials: Science and Engineering*. Springer. p. 27. ISBN 0-387-46270-8.
- [15] Richerson David W.; Freita Douglas W. "Ceramic Industry". *Opportunities for Advanced Ceramics to Meet the Needs of the Industries of the Future* (1998). Oak Ridge National Laboratory. OCLC 692247038.
- [16] Riley F. L. "Silicon Nitrides: An Overview." *Science of Ceramics* 12 (1983): 15.
- [17] Mazzocchi M; Bellosi, A (2008). "On the possibility of silicon nitride as a ceramic for structural orthopaedic implants. Part I: Processing, microstructure, mechanical properties, cytotoxicity". *Journal of Materials Science: Materials in Medicine*. 19 (8): 2881–7. doi:10.1007/s10856-008-3417-2. PMID 18347952.
- [18] Koskinen J., & Johnson H. (1988). *Silicon Nitride Fibers Using Micro Fabrication Methods*. MRS Proceedings, 130. doi:10.1557/PROC-130-63.
- [19] Li Xiang, Guangqing Zhang, Ragnar Tronstad, and Oleg Ostrovski. "Synthesis of SiC whiskers by VLS and VS process." *Ceramics International* 42, no. 5 (2016): 5668-5676.
- [20] Zhang Yong, Ruying Li, Xiaorong Zhou, Mei Cai and Xueliang Sun. "Selective growth of  $\alpha$ -Al<sub>2</sub>O<sub>3</sub> nanowires and nanobelts." *Journal of Nanomaterials* 2008 (2008): 20.
- [21] Miguel A. Rodriguez, Nikolay S. Makhonin, Juan A. Escrilia, Inna P. Borovinskaya, Maria I. Osendi, Maria E Barba, Juan E. Iglesias, and Josi S. Moya, Si<sub>3</sub>N<sub>4</sub> Fibers Obtained by Self-propagating High Temperature Synthesis, *Adv Mater* 1995, 7. No 8.
- [22] Yang Li, Jiacheng Gao, Preparation of silicon nitride ceramic fibers from polycarbosilane fibers by  $\gamma$ -ray irradiation curing, *Materials Letters* 110 (2013) 102–104.
- [23] Wang F, Jin G Q, Guo X Y. Formation mechanism of Si<sub>3</sub>N<sub>4</sub> nanowires via carbothermal reduction of carbonaceous silica xerogels[J]. *The Journal of Physical Chemistry B*, 2006, 110(30): 14546-14549.
- [24] Frieser, R. G. "Direct nitridation of silicon substrates." *J. Electrochem. Soc.* 115 (1968): 1092-1094.
- [25] Mitomo M. "Effect of Fe and Al additions on nitridation of silicon." *Journal of Materials Science* 12.2 (1977): 273-276.
- [26] Pavarajarn Varong and Shoichi Kimura. "Catalytic effects of metals on direct nitridation of silicon." *Journal of the American Ceramic Society* 84.8 (2001): 1669-1674.
- [27] Boyer S. M. and A. J. Moulson. "A mechanism for the nitridation of Fe-contaminated silicon." *Journal of Materials Science* 13, no. 8 (1978): 1637-1646.

- [28] Yin Shao-wu, Li Wang, Li-ge Tong, Fu-ming Yang and Yan-hui Li. "Kinetic study on the direct nitridation of silicon powders diluted with  $\alpha$ -Si<sub>3</sub>N<sub>4</sub> at normal pressure." *International Journal of Minerals, Metallurgy, and Materials* 20, no. 5 (2013): 493-498.
- [29] Kamimura Seiji, Tadao Seguchi and Kiyohito Okamura. "Development of silicon nitride fiber from Si-containing polymer by radiation curing and its application." *Radiation Physics and Chemistry* 54.6 (1999): 575-581.
- [30] Xu Xin, et al. "Synthesis and Photoluminescence of Eu<sup>2+</sup>-Doped  $\alpha$ -Silicon Nitride Nanowires Coated with Thin BN Film." *Journal of the American Ceramic Society* 90.12 (2007): 4047-4049.
- [31] Wang Zhihao, et al. "Synthesis and photoluminescence of heavily La-doped  $\alpha$ -Si<sub>3</sub>N<sub>4</sub> nanowires via nitriding cyromilled nanocrystalline La-doped silicon powder." *Journal of Luminescence* 151 (2014): 66-70.
- [32] Yingjiu Zhang, et al. "A simple method to synthesize Si<sub>3</sub>N<sub>4</sub> and SiO<sub>2</sub> nanowires from Si or Si/SiO<sub>2</sub> mixture." *Journal of Crystal Growth* 233 (2001) 803–808
- [33] Ahmad, Mashkoor, et al. "One-step synthesis route of the aligned and non-aligned single crystalline  $\alpha$ -Si<sub>3</sub>N<sub>4</sub> nanowires." *Science in China Series E: Technological Sciences* 52.1 (2009): 1-5.
- [34] Saulig-Wenger Karine, et al. "Synthesis and Characterization of Cubic Silicon Carbide ( $\beta$ -SiC) and Trigonal Silicon Nitride ( $\alpha$ -Si<sub>3</sub>N<sub>4</sub>) Nanowires." *Developments in Advanced Ceramics and Composites: Ceramic Engineering and Science Proceedings, Volume 26, Number 8 (2005):* 341-348.
- [35] Liang Feng, et al. "Catalytic Effects of Cr on Nitridation of Silicon and Formation of One-dimensional Silicon Nitride Nanostructure." *Scientific Reports* 6 (2016).
- [36] Zhang Xiaoguang, et al. "Preparation and characterization of the properties of polyethylene glycol@ Si<sub>3</sub>N<sub>4</sub> nanowires as phase-change materials." *Chemical Engineering Journal* 301 (2016): 229-237.
- [37] Wang Feng, et al. "Effects of the reaction conditions in preparation of Si<sub>3</sub>N<sub>4</sub> nanowires." *Acta Physico-Chimica Sinica* 23.10 (2007): 1503-1507.
- [38] Liu Ji-Xuan, et al. "Properties of porous Si<sub>3</sub>N<sub>4</sub>/BN composites fabricated by RBSN technique." *International Journal of Applied Ceramic Technology* 7.4 (2010): 536-545.
- [39] Li Gong-Yi, et al. "Long silicon nitride nanowires synthesized in a simple route." *Applied Physics A: Materials Science & Processing* 93.2 (2008): 471-475.

- [40] Ahmad Mashkour, et al. "Ordered arrays of high-quality single-crystalline  $\alpha$ -Si<sub>3</sub>N<sub>4</sub> nanowires: synthesis, properties and applications." *Journal of Crystal Growth* 311.20 (2009): 4486-4490.
- [41] Liu Haitao, et al. "Novel, low-cost solid-liquid-solid process for the synthesis of  $\alpha$ -Si<sub>3</sub>N<sub>4</sub> nanowires at lower temperatures and their luminescence properties." *Scientific reports* 5 (2015).
- [42] Wang Qiushi, et al. "Epitaxial growth of asymmetric  $\alpha$ -silicon nitride nanocombs." *Materials Research Bulletin* 45.7 (2010): 888-891.
- [43] Huang Juntong, et al. "Co-catalyzed nitridation of silicon and in-situ growth of  $\alpha$ -Si<sub>3</sub>N<sub>4</sub> nanorods." *Ceramics International* 40.7 (2014): 11063-11070.
- [44] Xu Yajie, et al. "Preparation of novel saw-toothed and riblike  $\alpha$ -Si<sub>3</sub>N<sub>4</sub> whiskers." *The Journal of Physical Chemistry B* 110.7 (2006): 3088-3092.
- [45] Arik H., S. Saritas, and M. Gündüz. "Production of Si<sub>3</sub>N<sub>4</sub> by carbothermal reduction and nitridation of sepiolite." *Journal of materials science* 34.4 (1999): 835-842.
- [46] Jennings H. M. "Review on reactions between silicon and nitrogen." *Journal of Materials Science* 18.4 (1983): 951-967.
- [47] Watari Koji, et al. "Hot isostatic pressing to increase thermal conductivity of Si<sub>3</sub>N<sub>4</sub> ceramics." *Journal of materials research* 14.04 (1999): 1538-1541.
- [48] Yang Jian-Feng, Zhen-Yan Deng, and Tatsuki Ohji. "Fabrication and characterisation of porous silicon nitride ceramics using Yb<sub>2</sub>O<sub>3</sub> as sintering additive." *Journal of the European Ceramic Society* 23.2 (2003): 371-378.
- [49] Xu Zhaoyun, et al. "Preparation of Porous Si<sub>3</sub>N<sub>4</sub> Ceramics with Controlled Porosity and Microstructure by Fibrous  $\alpha$ -Si<sub>3</sub>N<sub>4</sub> Addition." *Journal of the American Ceramic Society* 97.11 (2014): 3392-3395.
- [50] Fukasawa Takayuki, et al. "Synthesis of Porous Silicon Nitride with Unidirectionally Aligned Channels Using Freeze-Drying Process." *Journal of the American Ceramic Society* 85.9 (2002): 2151-2155.
- [51] Stucker Brent. "Additive manufacturing technologies: technology introduction and business implications." In *Frontiers of Engineering: Reports on Leading-Edge Engineering From the 2011 Symposium*, National Academies Press, Washington, DC, Sept, pp. 19-21. 2012.
- [52] Frazier William E. "Metal additive manufacturing: a review." *Journal of Materials Engineering and Performance* 23.6 (2014): 1917-1928.
- [53] Lipson Hod and Melba Kurman. *Fabricated: The new world of 3D printing*. John Wiley & Sons, 2013.

- [54] Conner Brett P., Guha P. Manogharan, Ashley N. Martof, Lauren M. Rodomsky, Caitlyn M. Rodomsky, Dakesha C. Jordan, and James W. Limperos. "Making sense of 3-D printing: Creating a map of additive manufacturing products and services." *Additive Manufacturing* 1 (2014): 64-76.
- [55] Lee Jian-Yuan, Jia An and Chee Kai Chua. "Fundamentals and applications of 3D printing for novel materials." *Applied Materials Today* 7 (2017): 120-133.
- [56] Kruth Jean-Pierre, et al. "Binding mechanisms in selective laser sintering and selective laser melting." *Rapid prototyping journal* 11.1 (2005): 26-36.
- [57] Herzog Dirk, et al. "Additive manufacturing of metals." *Acta Materialia* 117 (2016): 371-392.
- [58] EOS Electro Optical Systems GmbH, [www.eos.info](http://www.eos.info).
- [59] Concept Laser GmbH, [www.concept-laser.com](http://www.concept-laser.com).
- [60] Kannan Ganesa Balamurugan, and Dinesh Kumar Rajendran. "A Review on Status of Research in Metal Additive Manufacturing." *Advances in 3D Printing & Additive Manufacturing Technologies*. Springer Singapore, 2017. 95-100.
- [61] Kruth Jean-Pierre, et al. "Binding mechanisms in selective laser sintering and selective laser melting." *Rapid prototyping journal* 11.1 (2005): 26-36.
- [62] SLM Solutions GmbH, [www.slm-solutions.com](http://www.slm-solutions.com).
- [63] Marina Aghayan, Irina Hussainova, Fabrication of NiO/NiAl<sub>2</sub>O<sub>4</sub> nanofibers by combustion method. *Key Engineering Materials* Vol. 674 pp 31-34 (2016)
- [64] ASTM E9-09, Standard Test Methods of Compression Testing of Metallic Materials at Room Temperature, ASTM International, West Conshohocken, PA, 2009, [www.astm.org](http://www.astm.org)
- [65] Metallos, Department of Materials Science & Metallurgy, University of Cambridge, 24 October 2007, [wikimedia.org/wiki/File:Ellingham-diagram-greek.svg](http://wikimedia.org/wiki/File:Ellingham-diagram-greek.svg)
- [66] H.M. Jennings, Review on reactions between silicon and nitrogen, *J. Mater. Sci.* 18 (1983) 951–967.
- [67] Melting points table of the elements, CHEMIX School - Portable Chemistry Software, Last updated: Apr 21, 2017
- [68] A. Malecki and J. P. Doumerc, Kinetics of thermal decomposition of Co<sub>3</sub>O<sub>4</sub> powder and single crystals , *Journal of Thermal Analysis*, Vol. 36, 215- 222(1990)

## **ACKNOWLEDGEMENTS**

This thesis is based on the experimental work carried out at the School of Engineering, Tallinn University of Technology.

First, I want to thank my supervisor professor Irina Hussainova, for her excellent guidance, continuous support and fruitful discussions during my research work.

I want to thank the member of the research group who have contributed to my thesis: for their continuous help and support.

Last, I want to thank my family members and friends for your support that I could finish my thesis.